

Luca Saba

*Prediction is very difficult especially about the future*

*Niels Bohr (1885–1962)*

*Atomic Theory and the Description of Nature 1934*

## Contents

<b>13.1</b>	<b>Introduction</b> .....	285
<b>13.2</b>	<b>Technical Considerations</b> .....	286
13.2.1	Computed Tomography .....	286
13.2.2	Magnetic Resonance .....	290
13.2.3	Ultrasonography.....	292
13.2.4	Other Techniques .....	293
<b>13.3</b>	<b>Imaging of Carotid Arteries</b> .....	295
13.3.1	Introduction.....	295
13.3.2	Imaging Diagnostic Flow Chart.....	295
13.3.3	From Stenosis Degree to Vulnerable Plaque.....	295
13.3.4	Carotid Artery Stenosis Quantification.....	296
13.3.5	Carotid Artery Plaque Characterization.....	297
<b>13.4</b>	<b>Central Vessels</b> .....	301
13.4.1	Aorta .....	301
13.4.2	Pulmonary Arteries .....	304
<b>13.5</b>	<b>Peripheral Vessels</b> .....	306
13.5.1	Lower Extremities.....	306
13.5.2	Upper Extremities .....	309
<b>References</b> .....		311

## Abbreviations

AAA	Abdominal aortic aneurysms
CE-MRA	Contrast-enhanced magnetic resonance angiography
CT	Computed tomography
CTA	Computed tomography angiography
DP	Dorsalis pedis
DSA	Digital subtraction angiography
DVT	Deep venous thrombosis
HU	Hounsfield units
MDCTA	Multi-detector-row CT angiography
MOTSA	Multiple overlapping thin slab acquisitions
MR	Magnetic resonance
MRA	Magnetic resonance angiography
MRI	Magnetic resonance imaging
PE	Pulmonary embolism
PT	Posterior tibial
TOF	Time of flight

## 13.1 Introduction

Aging is responsible for several changes in the heart and blood vessels (Minaker 2007; Schwartz and Zipes 2007). Aging causes changes in the structure and composition of the blood vessels that lead to an increase in the incidence of cardiovascular diseases, such as cerebrovascular disease, hypertension, coronary artery disease, heart failure, and postural hypotension with enhancement of both morbidity and mortality (Jefferson et al. 2011; Towfighi and Saver 2011; Butler et al.

---

L. Saba, MD  
Department of Radiology,  
Azienda Ospedaliero Universitaria,  
SS 554 Monserrato (CA), Italy  
e-mail: lucasaba@tiscali.it

2011). It is well demonstrated that aging is responsible for important changes in vascular structure and function, which in turn affect the function of the heart and other organs. One of the main hallmarks of aging is large artery remodeling, which results in a progressive increase in wall thickness and lumen enlargement. Aging is almost always accompanied by atherosclerosis in humans, but these two processes differ in many aspects.

Aging is a physiological process that affects the entire vascular system, starts after sexual maturation, and leads to enlargement of the lumen of large arteries, whereas atherosclerosis is a disease that affects limited areas of the arterial tree and tends to narrow the lumen in adults. Vascular aging is characterized by degenerative processes, alterations in endothelial function, and arterial stiffening. These changes can reflect adaptive or degenerative processes.

The mechanism responsible for arterial remodeling is still a matter of debate, but it seems to involve disorganization of the extracellular matrix. Arterial aging is associated with extensive quantitative and qualitative changes affecting elastin. Elastase activity was found to be increased in the plasma and arterial walls of old individuals, which could account for some of the observed alterations of elastic fibers (Robert et al. 1984). Authors demonstrated that elastic fibers from old animals and humans (Cliff 1970; Fornieri et al. 1992; O'Rourke et al. 1987) are disorganized, thinner, and more fragmented in comparison with those of younger individuals. Anidjar et al. (1990) found that elastic fibers have a major support role in the arteries, and experimental alterations of elastin result in arterial dilation and formation of aneurysms.

Another important feature of age-related remodeling is the thickening of the intimal layer (Gerrity and Cliff 1972; Guyton et al. 1983). In the human aorta, a two- to sixfold increase in intima thickness between the ages of 20–40 and 65 years or more has been evidenced (Virmani et al. 1991). Compared with the young intima, the aged intima contains higher amounts of collagen, glycosaminoglycans, fragmented elastic fibers, smooth muscle

cells, and other mononuclear cells (Haudenschild et al. 1981; Richardson et al. 1988).

In the carotid arteries, these pathologic changes determine the development of the plaque that is the main cause of ischemic stroke of the brain (Gao et al. 2009). In the past the degree of stenosis determined by the carotid plaque was considered the main risk factor for the development of cerebrovascular events (Kolodgie et al. 2007; Weinberger 2002), but in recent years, the concept that the degree of luminal obstruction alone is insufficient to predict a plaque's vulnerability has been introduced, thus the concept of "vulnerable plaque." Vulnerable plaques are atherosclerotic plaques that have a high likelihood to cause thrombotic complications, such as myocardial infarction or stroke (Naghavi et al. 2006; Casscells et al. 2003).

The challenge for imaging techniques is to identify patients with pathologic changes of the vessels and those high-risk patients with vulnerable plaques, before any adverse event occurs.

This chapter will discuss the capabilities of various imaging techniques in the identification and characterization of the pathology of the central and peripheral vessels.

---

## 13.2 Technical Considerations

In recent years the technical evolution of imaging modalities like CT, MR, and ultrasound have provided excellent results for the analysis and characterization of vascular pathology. In particular, with the development of extremely fast volumetric CT scanners, it is nowadays possible to visualize the carotid arteries and the circle of Willis in a few seconds. In this section the modern imaging techniques will be analyzed by explaining their capabilities and potential clinical applications.

### 13.2.1 Computed Tomography

#### 13.2.1.1 Introduction

CT angiography (CTA), in particular multi-detector-row CTA (MDCTA), is a powerful non-invasive imaging tool (Fig. 13.1). In the last

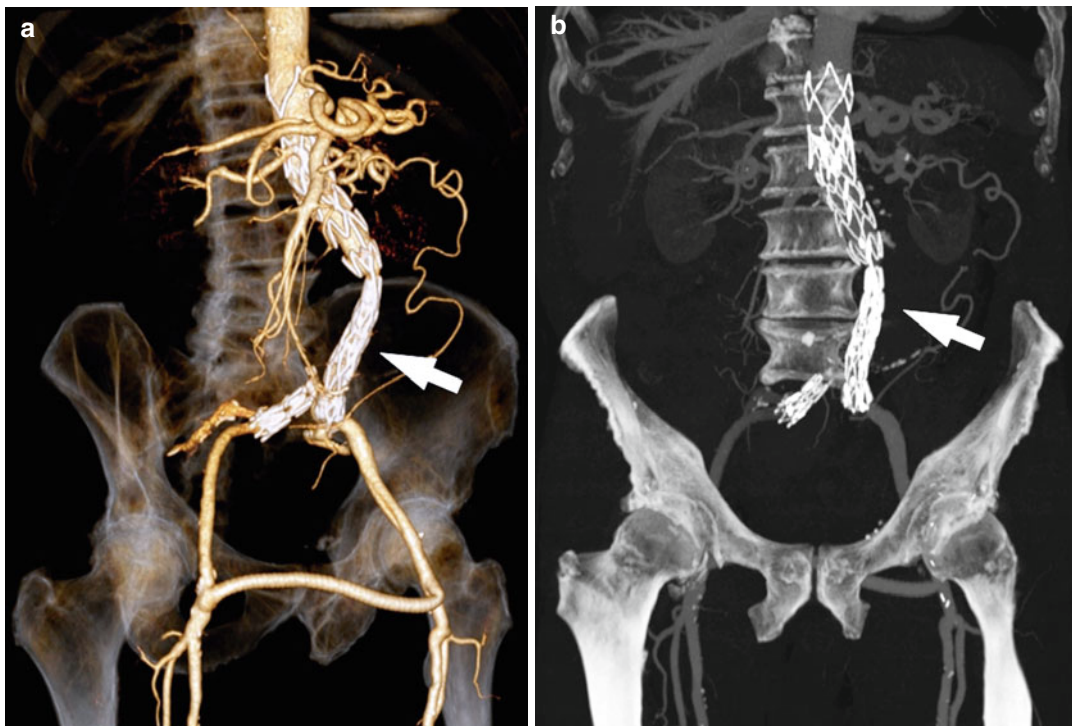


**Fig. 13.1** MDCTA images. Volume-rendered (a) and maximum-intensity projection (b) post-processed CTA images show a bypass between the femoral arteries (*white*

*arrow*) in a 67-year-old patient. Also visible is the presence of an endovascular stent graft in the abdominal aorta and common iliac arteries

15 years, CT has experienced tremendous technological development. The first generation of CT scanners was developed in the 1970s (Prokop 2003; Walter et al. 2004). Numerous innovations have improved the utility and application of CT, in particular the introduction of helical CT systems that allowed the development of the “volumetric CT” concept.

In the first- and second-generation scanner (sequential scanner), the scan volume was covered in a stepwise manner: The table, after acquiring an axial section, was moved and the next scan was performed. The most important limitation of this type of scanning technique was that it was extremely slow. A major improvement in the CT technology was the incorporation of continuously rotating X-ray tubes with a single-detector row longitudinally positioned in the gantry. This was the introduction of third-generation geometry (spiral CT). With these scanners, an X-ray tube and a detector array rotate synchronously and

continuously around the patient, and it became possible to acquire volume data of the patient. This technique is the basis of CTA because it allows rapid and continuous imaging of a large volume so that the contrast enhancement is present only in the arteries and not in the veins.

In 2001 the introduction of 16-slice CT scanners finally allowed isotropic CT scanning with the ability to produce 1,000 images in less than 15 s. As compared to 4-detector-row scanners, performance of 32- to 64-detector-row scanners has increased more than 20 times owing to more detector rows and faster rotation speed. A recent important improvement in the CT technology is the introduction of the dual source CT (Wintermark et al. 2008a; Fishman 2003).

Nowadays, isotropic voxels, high spatial and temporal resolution, and use of fast contrast material injection rate and post-processing tools improved sensitivity and specificity of MDCTA. This technique allows full vascular imaging in a

few seconds from the aorta to the circle of Willis. For instance, examination of the whole length of the carotid arteries from the aortic arch to the circle of Willis requires only a 2-s scan time with a 128-detector-row CT ( $64 \times 0.6$  mm, pitch of 1.33, 0.33-s rotation time).

### 13.2.1.2 Principles

CT is an X-ray technique in which an X-ray source rotates around an object and the X-ray passes through the object from various directions. The X-ray attenuation along each of the many paths through the object is analyzed by a mathematical image reconstruction (inverse Radon transformation) to calculate the local attenuation coefficient at each point within the acquisition volume. After this phase the local attenuation coefficients are normalized to yield CT numbers for every point of the matrix. At the end of the process, these CT numbers are converted into shades of grey.

In the use of the MDCTA, a fundamental step is to understand the scanning parameters. It is possible to identify three major categories: (1) acquisition parameters, (2) derivative parameters, and (3) reconstruction parameters. The acquisition parameters are the following: number of active detector rows, section collimation, rotation time, table feed per rotation, pitch factor, scan length, tube voltage, and tube load. Among these the section collimation is extremely important: it is determined by the total width of the acquired volume in the center of the scan field divided by the number of sections. The derivative parameters are the following: table speed (which is determined by the ratio of table feed and rotation time) and scan duration (measured in seconds and determined by the ratio of scan length and table speed). The reconstruction parameters are the following: field of view (FOV), matrix size, reconstruction filter, section thickness, and reconstruction interval. The FOV determines which part of the data will end up in the images, and the matrix size is the limiting factor for spatial resolution. Decreasing the matrix can reduce spatial resolution, but a very large matrix size cannot increase resolution beyond the inherent system resolution.

### 13.2.1.3 Image Processing

The latest generation of CT systems allows for isotropic imaging, and as a consequence, the distinction between transverse and in-plane resolution is gradually becoming a historical remnant, and the traditional axial slice is losing its clinical predominance. In fact it is now replaced by interactive viewing manipulation of isotropic volume images. Image processing and three-dimensional reconstruction of diagnostic images represent a necessary tool for depicting complex anatomical structures and understanding pathological changes in terms of both morphology and function.

In studying the vascular system with MDCT, it is possible to use different post-processing techniques. Projectional methods project a 3D volume into a bidimensional plane: multiplanar reformations (MPR), maximum-intensity projection (MIP), and minimum-intensity projection (MinIP). The perspective methods display a 3D virtual model with techniques that aim to reproduce the perspective of the human eye: shaded surface display (SSD) and volume rendering (VR).

The maximum-intensity projection (MIP) (Fig. 13.2) technique simulates rays that are traced from the radiologist through the object to the display screen, and only the relative maximum value detected along each ray path into the selected slab is considered in the algorithm of visualization; in this technique, only the voxel with the highest CT number is displayed, depending on the voxel position along the projecting ray (Prokop et al. 1997). With MIP it is possible to obtain images similar to digital subtraction angiography (DSA), but with this technique, there are some artifacts that radiologists need to be aware of: in particular a high density structure (e.g., calcification) may obscure information from intravascular contrast material. Therefore, mural plaque calcifications may obscure the lumen and may lead to an overestimation of the degree of luminal stenosis.

Multiplanar reformations (MPR) (Fig. 13.2) provide images that can be oriented in every spatial direction by using arbitrary chosen views; this technique is mainly used for quantitative lumen analysis because it can depict the lumen shape.



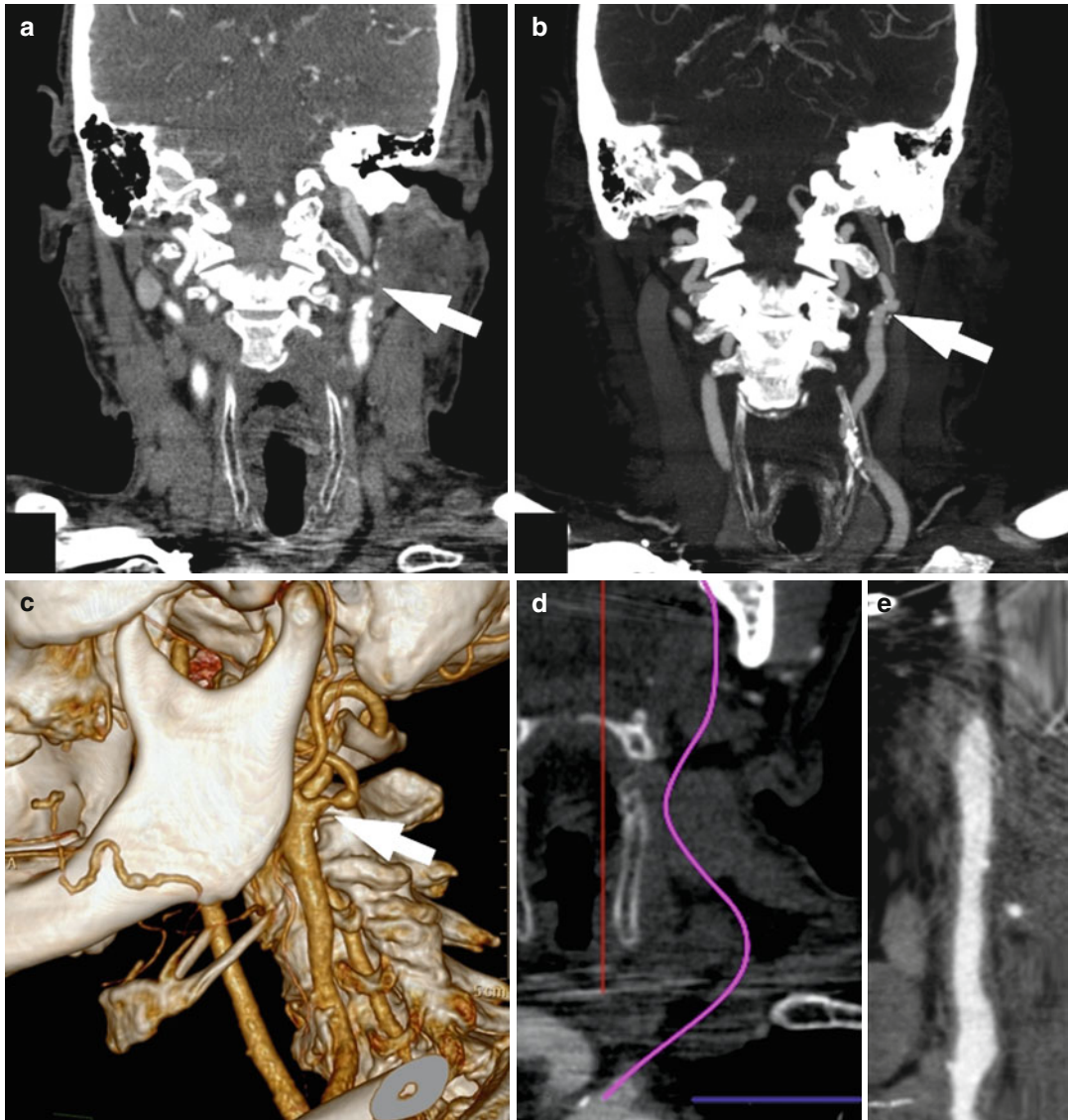


**Fig. 13.2** MDCTA post-processing techniques. CTA images in a 74-year-old patient who suffered a left transient ischemic attack. Different post-processing techniques demonstrated the presence of the stenosis in the left internal

carotid artery (*white arrow*). Multiplanar reconstruction (**a**), maximum-intensity projection (**b**), volume rendering, (**c**) and curved planar reconstruction (**d**, **e**)

Curved plane reconstruction *or* CPR (Fig. 13.2) is another two-dimensional post-processing method that shows the cross-sectional profile of a vessel along its length (Calhoun et al. 1999; Rankin 1998; Rubin et al. 1995). This technique is frequently used in the analysis of vessels because they commonly have curvilinear morphology that

oblique reformations cannot capture. Some authors consider CPR a variation of MPR.

Volume rendering (VR) (Fig. 13.2) incorporates all CT raw data to produce high-quality three-dimensional images. The purpose of VR algorithms is to represent and analyze volume data in a realistic way by integrating a series of

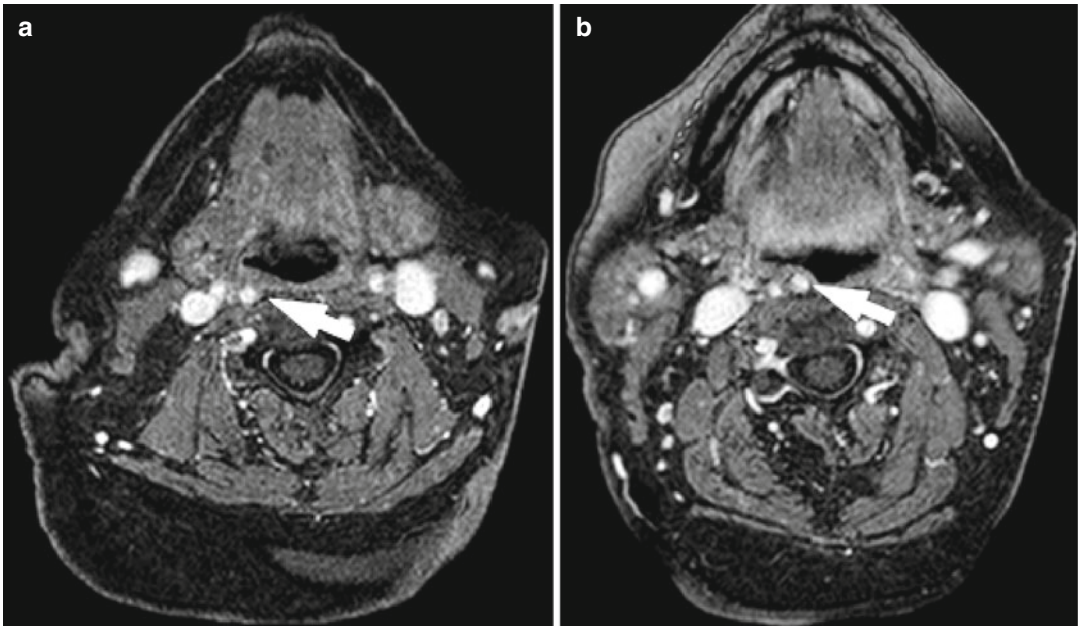


**Fig. 13.3** MRI of carotid arteries. MRI of a 71-year-old patient who suffered right amaurosis. Images show the right internal carotid artery (*white arrow*). These images clearly show the anatomical course of the neck vessels

axial CT sections into a form that is easier to interpret than the original images.

## 13.2.2 Magnetic Resonance

### 13.2.2.1 Introduction

In recent years, MR has become a fundamental method to evaluate vascular pathology. With the use of different acquisition techniques, it is possible to obtain information to quantify, identify, and characterize the pathology that affects the vessels (Fig. 13.3). In particular, in the last decade, significant progress has been made towards non-invasive detection of vulnerable atherosclerotic plaques using MR angiography (MRA) (Saam et al. 2007; Briley-Saebo et al. 2007). This imaging technique does not involve ionizing radiation and enables visualization of the vessel lumen (Choudhury et al. 2002; Yuan et al. 2001). The first application of MR to the vascular system started in the mid-1980s (Alvarez et al. 1986; Wehrli et al. 1986), and in the last years, there have been significant improvements thanks to the increase of the magnetic field strength (from 0.3

to 3 T and more), the development of coils dedicated to carotid artery analysis (surface coils), the creation of advanced sequences for the data acquisition (black-blood techniques, time of flight), and the use of contrast material that improves the visualization of the vessel lumen.

The first MRA method, phase-contrast MRA was quickly followed by (2D) and 3D time-of-flight (TOF) MRA. TOF MRA has been widely adopted for an array of clinical indications but is relatively insensitive to slow flow and is associated with long scan times and signal voids, all of which can lead to poor-quality imaging and overestimation of stenosis. More recently, contrast-enhanced (CE) MRA has been introduced. CE-MRA produces high-quality images in a very short time and may alleviate some of the drawbacks associated with TOF MRA.

Since atherosclerotic disease affects the entire arterial system, it is desirable to extend coverage, allowing concomitant assessment of the arterial system from the carotid arteries to the distal runoff vessels. The implementation of “bolus chase” techniques extended coverage to encompass the entire runoff vasculature, including the pelvic,

femoral, popliteal, and trifurcation arteries. It is important to underline that MRA, however, is sensitive to artifacts caused by slow and turbulent flow associated with high-grade stenosis. For reliable diagnostic results, physicians and radiologists must be familiar with the different acquisition techniques.

### 13.2.2.2 Principles

MRI has emerged to be one of the major noninvasive methods for the evaluation of the vascular system. Most imaging of the vessel analysis by MRI has been performed on 1.5 T scanners. Recently, 3.0 T scanners and their resulting high-resolution images have opened the field of vascular imaging to new potentials. MR imaging of the vascular bed is possible using non-contrast MRA and contrast MRA:

#### Non-contrast MRA with Time-of-Flight Sequences

Time-of-flight sequences are gradient-echo sequences acquired perpendicularly to the longitudinal axis of the vessels with extremely short repetition times (TR): the resulting difference in spin saturation between the moving protons in blood (unsaturated) and stationary tissues (completely suppressed) creates the “in-flow enhancement” that produces the angiographic effect used for ToF imaging (Fig. 13.4). To achieve the maximum possible difference in signal intensity between blood and stationary tissue and to avoid venous enhancement, TR should be calibrated based on flow velocity. Additional saturation pulses can be adopted to further suppress the intrinsic signal of these structures. It is possible to acquire ToF sequences by using 2D or 3D k-space sampling. Three-dimensional k-space sampling is known as MOTSA (multiple overlapping thin slab acquisitions), and it seems to be more accurate for the detection and grading of stenosis. One of the main limitations of ToF sequences is that at the site of tighter stenosis, blood flow may become turbulent, with slow-moving protons producing dephasing effects with unpredictable signal loss within vessel lumen, leading to stenosis overestimation.



**Fig. 13.4** MR Time of Flight (TOF). MRI in a 71-year-old patient who suffered right amaurosis. Image clearly depicts the arterial vascular system of the neck and the absence of the left internal carotid artery, from its origin to the circle of Willis

#### Contrast-Enhanced MRA with T1-Weighted 3D Gradient-Echo Sequences

CE-MRA is based on the principle of shortening the T1 relaxation time of blood by intravenously injecting Gd-chelate contrast agents. This causes a significant difference in signal intensity between flowing blood and stationary tissue at heavily T1-weighted arterial phase imaging, leading to the high signal intensity of blood on post-Gd T1-weighted sequences.

The magnitude of vascular enhancement depends on the concentration of contrast agent within the vascular bed during acquisition, and ideally imaging should be performed at the peak of vascular enhancement, when a maximum difference between signal intensity of the target vessel and the surrounding overlapping structures exists. An important difference of CE-MRA compared to ToF is that CE-MRA is less flow sensitive and therefore does not overestimate the degree of luminal stenosis as can happen in ToF



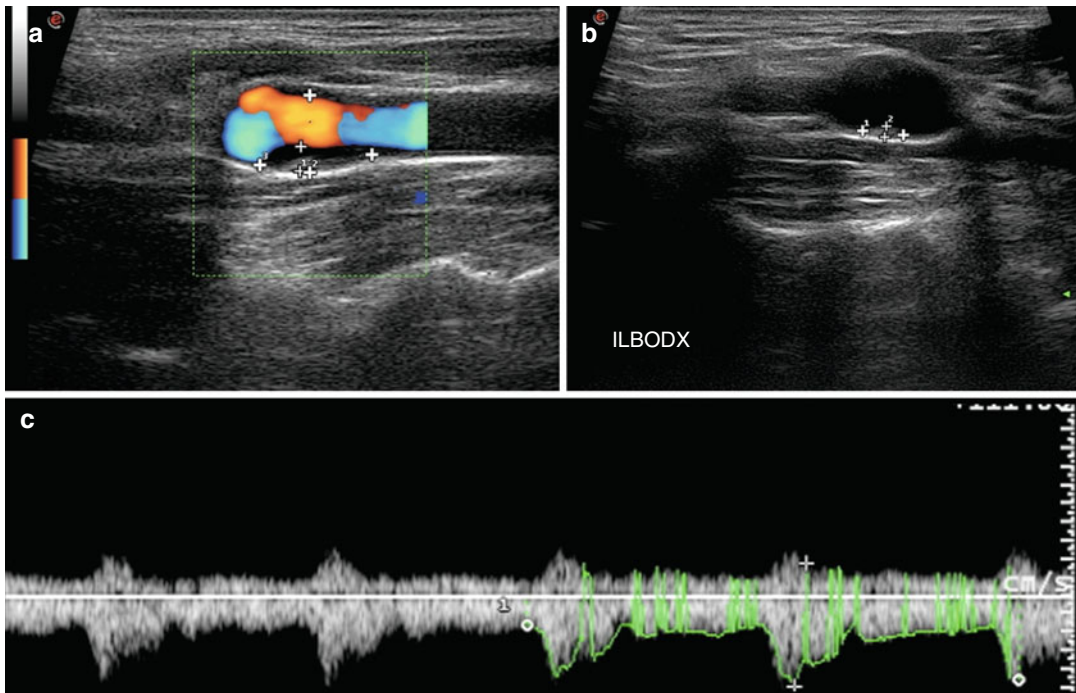


**Fig. 13.5** Ultrasound. Images demonstrate the presence of a small heterogeneous plaque in the right ICA (a, b). In panel c the spectra are given

sequences. The most relevant limitation of CE-MRA in the imaging of carotid arteries is that the arterial phase acquisition must be limited in duration to avoid the rapid onset of jugular enhancement, thus imposing relevant constraints to spatial resolution (Nederkoorn et al. 2003; Lenhart et al. 2002).

### 13.2.3 Ultrasonography

#### 13.2.3.1 Introduction

Ultrasonography is globally accepted as the standard imaging modality for first-line diagnosis of vascular pathology in all major vascular beds ranging from the carotid arteries to the arteries of the lower extremities. This high-resolution, noninvasive technique is readily available, rapidly applicable, and can be performed at relatively low cost (Fig. 13.5). High-frequency linear transducers (>7 MHz) are ideal to achieve high spatial resolution, whereas lower-frequency linear transducers

(<7 MHz) are preferred for Doppler examinations and analysis of central vessels like the aorta.

It has been widely demonstrated that ultrasound is a good screening technique even though some relevant limitations persist, in particular for the quantification of stenosis, including high operator and center variability, artifacts arising from calcifications, and difficulties in distinguishing subtotal occlusion from total occlusion.

#### 13.2.3.2 Principles

Ultrasonography of the carotid arteries is the modality of choice for triage, diagnosis, and monitoring of the pathology affecting peripheral vessels. This is an operator-dependent examination that requires a good understanding of Doppler physics and hemodynamic physiology. In fact the accuracy, sensitivity, and specificity of carotid ultrasound hinge on following standard guidelines and practicing meticulous scanning techniques because there are several pitfalls that may mislead the operator to falsely interpret color and spectral Doppler findings.



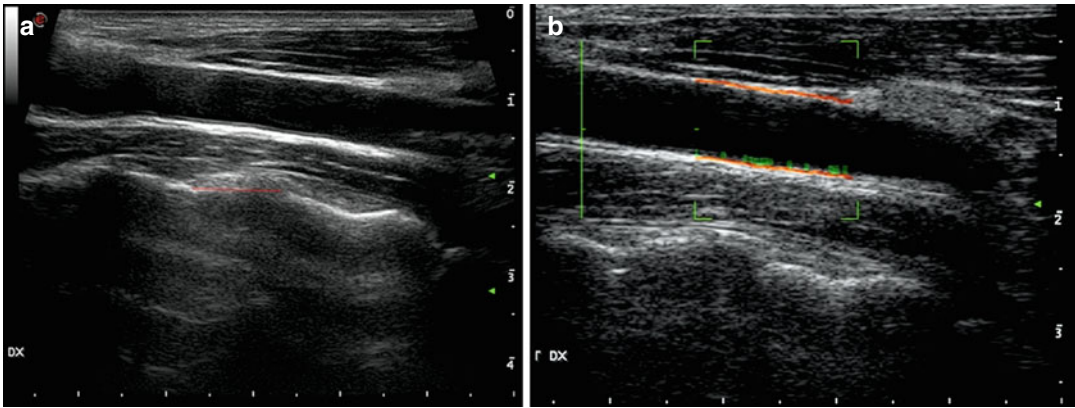


**Fig. 13.6** Intima-media thickness. Intima-media thickness in a 36-year-old patient (a); panel b shows an automated system for automatically detecting the intima-media thickness

Two main type of analysis can be performed by ultrasound: Doppler ultrasound and B-mode (morphological) ultrasound. The Doppler analysis evaluates the velocity of the flowing blood and is very useful in analysis of the atherosclerotic disease of carotid arteries as well as of iliac, femoral, popliteal, and tibial arteries. In this kind of exam, the angle theta affects the detected Doppler frequencies. In particular in the carotid artery analysis, at a Doppler angle of  $0^\circ$ , the maximum Doppler shift will be achieved since the cosine of  $0^\circ$  is 1. Conversely, no Doppler shift (no flow) will be recorded if the Doppler angle is  $90^\circ$  since the cosine of  $90^\circ$  is 0. It is possible to visualize the Doppler frequencies in a morphological way by using the color Doppler. In the analysis of the vascular system, and in particular for carotid and vessels of the lower extremities, Doppler is very useful because it allows quantification of the blood velocity. B-mode ultrasound is mainly used for the analysis of the carotid artery where identification and characterization of the plaque represent an important step in defining the risk of cerebrovascular event.

One of the most used applications of ultrasound is the identification and quantification of the so-called intima-media thickness, which is considered a measurable index for the presence of atherosclerosis (Fig. 13.6).

### 13.2.4 Other Techniques

Digital subtraction angiography (DSA) (Fig. 13.7) was considered the gold standard imaging reference for the evaluation of vascular pathology. However, its diagnostic role has been widely criticized for the limited number of views, costs, and the small but definite risk of complications. Nowadays in most institutions, where adequate CT and/or MR technology is available, the diagnostic use of DSA is limited to a small number of cases in which there is no agreement between two or more noninvasive tests. Instead, DSA procedures are only performed when endovascular treatment is needed.

Recently, other techniques have emerged that allow identification and characterization of pathology that may affect the body vessels. In particular positron emission tomography (PET) and optical coherence tomography (OCT) should be cited. In recent years a variety of studies have been performed with the intent to assess the diagnostic potential of  $^{18}\text{F}$ -FDG PET in the quantification of plaque inflammation: based on the assumption that unstable, inflamed plaques are infiltrated by lymphocytes and macrophages and that this latter cell population can absorb  $^{18}\text{F}$ -FDG from the interstitial spaces,  $^{18}\text{F}$ -FDG PET can be used to directly detect plaque inflammation in various anatomic locations (Tawakol et al. 2006).

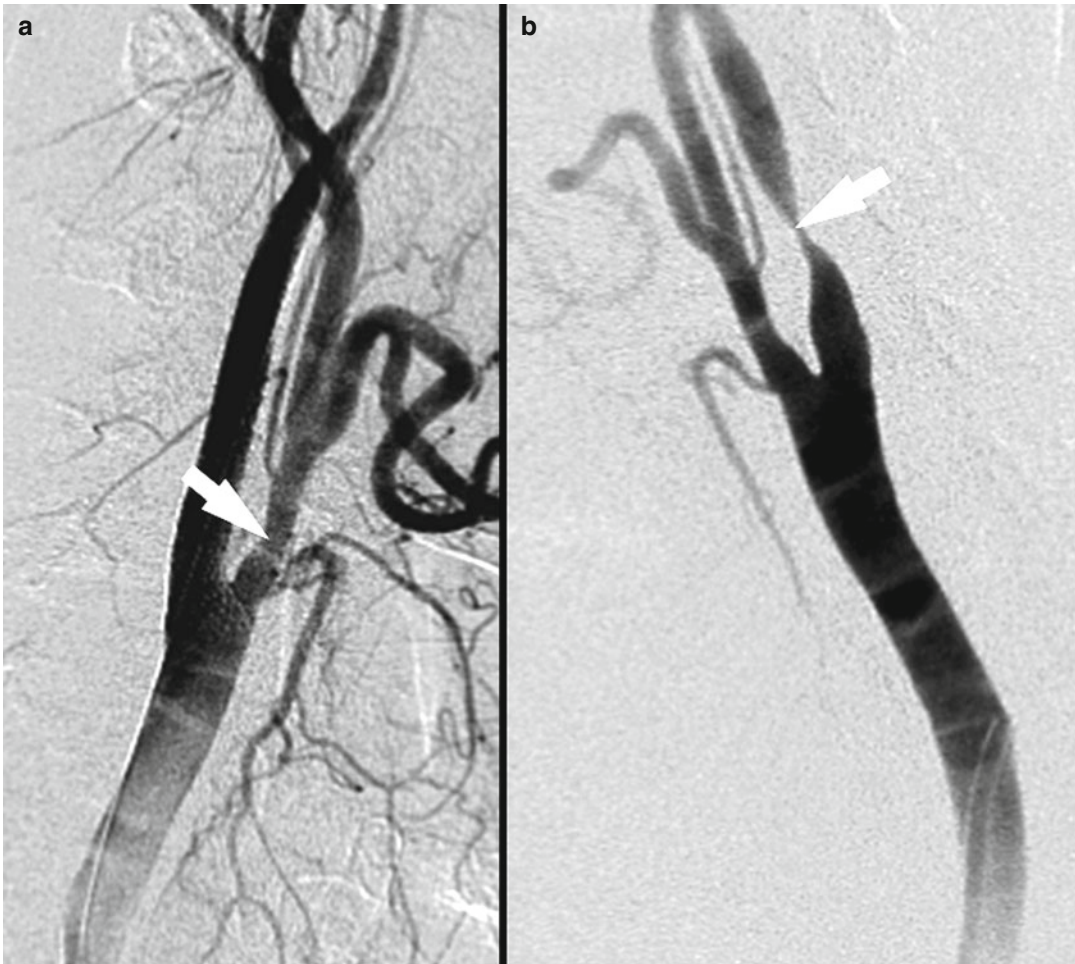


**Fig. 13.7** Digital subtraction angiography images. In *panel a* 30 % NASCET stenosis is visible; *panel b* shows a NASCET stenosis of 80 %, *arrows* indicates point of maximum stenosis

Molecular imaging is a new and revolutionary field. The development of multimodal, multi-functional nanoparticles, in particular when imaging the carotid arteries, is a growing field which can help our understanding of the underlying disease processes and which might help to improve the treatment of vascular diseases. During the development of atherosclerosis, complex interactions take place at the molecular and cellular level, with various atherosclerosis-related biomarkers present at different stages of the disease progression.

Currently, a number of molecular markers have been evaluated for molecular imaging of atherosclerosis. These markers are known

components of atheromas in animal models with advanced atherosclerosis. Because of the limited imaging contrast from most of these biomarkers, external contrast agents that target certain biomarkers are introduced for different imaging modalities. Molecular imaging is used mainly in carotid artery plaque analysis because it allows one to study and characterize *in vivo* the presence and activity of a number of molecules and cells related to the atherosclerotic disease and inflammation process.

OCT is an optical signal acquisition method that can produce three-dimensional images with micrometer resolution from optical scattering media. OCT is an interferometric technique and

typically uses near-infrared light. This technique has been used in cardiology to help diagnose coronary artery disease (Tahara et al. 2010; Guagliumi et al. 2010; Guagliumi and Sirbu 2008)

---

## 13.3 Imaging of Carotid Arteries

### 13.3.1 Introduction

Carotid atherosclerosis is one of the major causes of ischemic stroke, one of the most common causes of death and disability in the world (Sacco et al. 2006). The microscopic alterations of the initial phase of this disease start during childhood, but usually carotid plaques remain asymptomatic until an advanced pathological stage is reached. In the 1980s and 1990s, the degree of carotid artery stenosis was considered the only determinant factor for treatment, while at present several other factors are considered potentially important markers for future cerebrovascular events, including plaque composition, presence and state of the fibrous cap, intra-plaque hemorrhage, plaque ulceration, and plaque location (Seeger et al. 1995; Saba et al. 2007a; Saam et al. 2006; Kullo et al. 1998).

Advanced plaque imaging techniques allow analysis of plaque morphology and its characteristics as well as the presence of plaque complications such as ulceration, hemorrhage, and thrombus. The ability to identify plaques that are more prone to fragment and embolize is now vital for the early diagnosis, prevention, and treatment of stroke and neurological side effects.

### 13.3.2 Imaging Diagnostic Flow Chart

The choice of a specific imaging modality to assess the carotid artery depends mainly on the clinical indication for imaging and the skills available in individual centers. In the past DSA was the most used imaging method for patients with suspected carotid artery pathology, but recently, with the development of noninvasive imaging techniques, DSA is less frequently used

(Saba and Mallarini 2009a). In 2008, authors proposed that for patients with a high likelihood of vascular disease, CTA may represent an appropriate first exam (Jaff et al. 2008; Libby 1998), whereas in patients with a low likelihood of vascular disease, ultrasound should be used. If pathology in the carotid arteries is found, CTA as well as MRA can be used to confirm the diagnosis and to accurately determine the precise degree of stenosis and to characterize the plaque composition. DSA is rarely necessary and only used in cases of severe multiple vessels disease, for which assessment of flow direction and collateral patterns may be important or when the image quality of noninvasive procedures is considered to be nondiagnostic.

### 13.3.3 From Stenosis Degree to Vulnerable Plaque

In the past, the degree of luminal stenosis in the carotid artery has been used as a direct measure of atherosclerosis severity (Fig. 13.8). However, studies in the coronary arteries showed that low stenosis degree may also lead to myocardial infarction (Jaff et al. 2008; Libby 1998; Fuster et al. 1990) and similar results were obtained in the carotid arteries (Lovett et al. 2004a, b). Since low-grade arterial stenosis can lead to cerebrovascular events, it appears important to look beyond the degree of stenosis at plaque morphology and composition.

Therefore, the concept of vulnerable plaque was introduced into surgical, histopathological, and imaging communities, referring to atheromas containing large necrotic cores covered by a thin or disrupted fibrous cap with a high tendency to rupture, embolize, and induce thrombus formation (Naghavi et al. 2003). Usually, major atherosclerotic alterations occur at the outer wall of the proximal segment and sinus of the internal carotid artery in the region of the lowest wall shear stress. In contrast, plaque thickness is lowest at the side of the flow divider at the junction of the internal and external carotid arteries where wall stress is the highest (Hardie et al. 2007).



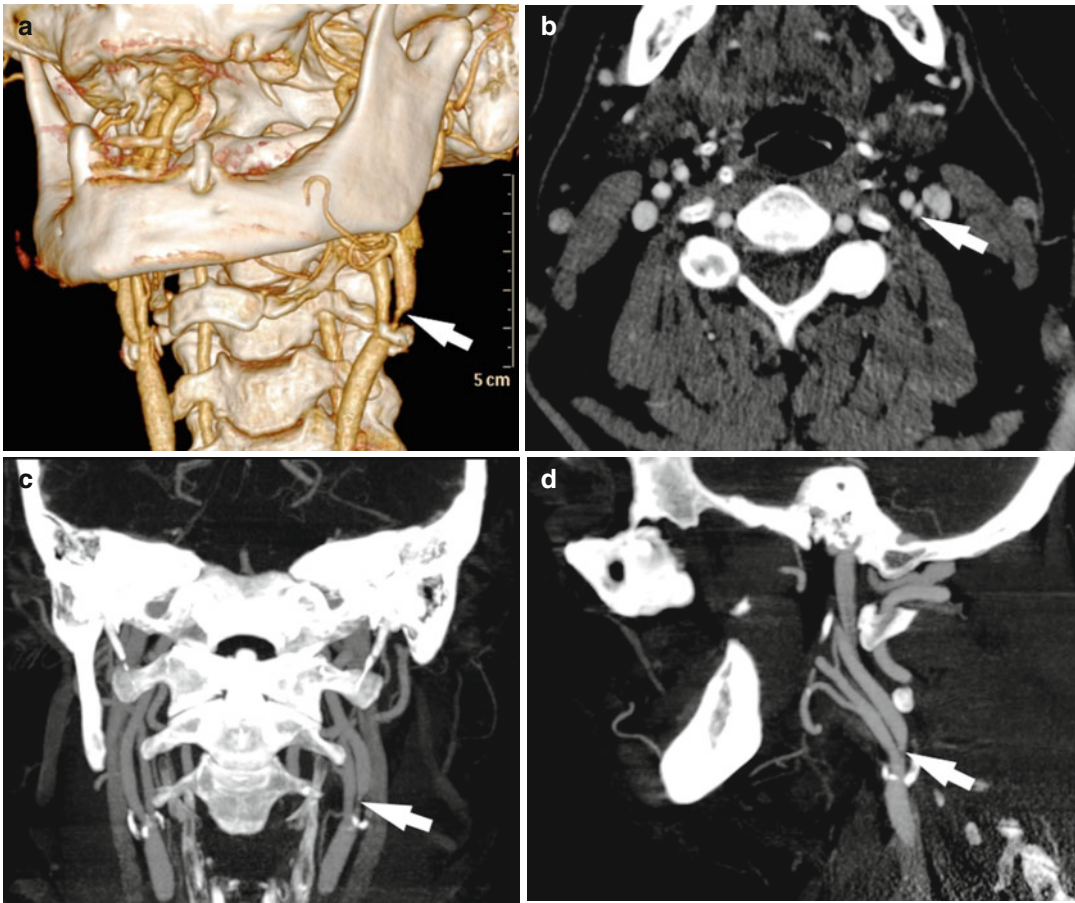


**Fig. 13.8** CTA stenosis detection. CT angiography in a 71-year-old patient who suffered a right transient ischemic attack. Volume rendering (a), axial (b), and

maximum-intensity projection (c, d) images show a 75 % NASCET stenosis, *arrows* indicate point of maximum stenosis

### 13.3.4 Carotid Artery Stenosis Quantification

The degree of stenosis is considered one of the most important parameters in the choice of the therapeutic option. In fact higher grades of carotid stenosis are associated with an increased risk of stroke. Three major methods for measuring carotid artery stenosis have been proposed: the North American Surgery Carotid Endarterectomy Trial (NASCET), the European Carotid Surgery Trial (ECST), and the Carotid Surgery Index (CSI) (North American Symptomatic Carotid Endarterectomy Trial Collaborators 1991; European Carotid Surgery Trialists' Collaborative Group 1998; Executive Committee for the

Asymptomatic Carotid Atherosclerosis Study 1995). These methods evaluate the degree of stenosis as the percentage reduction in the linear diameter of the artery. There are differences in the evaluation of the degree of stenosis among NASCET, ECST, and CSI, and values derived from these methods are not equal: it is always important to specify which classification is being used. NASCET is calculated by using the ratio between the lumen diameter at the site of the stenosis and the normal lumen diameter distally in a non-diseased reference segment. ECST is calculated as the ratio between the lumen diameter at the stenosis and the total carotid diameter at the same location. CSI is calculated by using the ratio between the lumen diameter at the site of



the stenosis and the normal lumen of the proximal common carotid artery multiplied by 1.2.

To quantify the degree of the stenosis, both NASCET and ECST measurements have to be performed on a plane exactly perpendicular to the carotid axis. Saba et al. demonstrated that NASCET and ECST show a strong correlation and that interobserver and intraobserver agreement values are high for both NASCET and ECST (Saba and Mallarini 2010a, b). Moreover NASCET, ECST, and CSI can be converted into each other with good results.

In the evaluation of carotid artery stenosis, ultrasound, CTA, and MRA are widely used. Nowadays, ultrasound is commonly performed to screen patients with possible carotid artery disease, but the accuracy of ultrasound echo-color Doppler is moderate if the purpose is the determination of the degree of stenosis (Eliaszewicz et al. 1995). In some institutions, the only diagnostic imaging test used for selecting patients for carotid endarterectomy is ultrasound, but this approach may lead to critical errors and has been widely criticized (Eliaszewicz et al. 1995; Polak et al. 1993; Goodson et al. 1987; Dawson et al. 1993).

Nowadays, CTA probably represents the best imaging method to quantify carotid artery stenosis: its sensitivity is comparable to angiography, but it is associated with fewer risks (Sameshima et al. 1999; Verhoek et al. 1999). In particular CTA sensitivity for stenosis between 70 and 99 % in internal carotid artery, using DSA as reference standard, can reach excellent results.

MRA has become widely used as a noninvasive diagnostic imaging modality for carotid artery stenosis quantification because it avoids the radiation and iodinated contrast exposure associated with CTA, and has a good sensitivity in the detection of the degree of stenosis (sensitivity of 93 % and a specificity of 88 %) associated with excellent potential to characterize plaque composition and morphology (Yucel et al. 1999). ToF is a very simple technique to image carotid arteries by using MRI, but it overestimates the degree of stenosis. CE-MRA offers better results, compared to ToF, but suffers one limitation: the inherent risks of administering the contrast material.

Recently new concepts have been proposed to quantify arterial stenosis in the atherosclerotic carotid artery; in particular with the introduction of MDCTA, thanks to its high spatial resolution (with isotropic voxels of 1 mm), a new direct millimeter method has been proposed by Bartlett and colleagues (Bartlett et al. 2006a, b, 2007) to overcome limitations of the classical percent methods like NASCET, ECST, and CSI. The authors showed that threshold values of 1.4–2.2 mm can be used to evaluate for moderate stenosis (50–69 % according to NASCET) with a sensitivity of 75 % and a specificity of 93.8 %, whereas a diameter of 1.3 mm corresponds to 70 % stenosis with a sensitivity of 88 % and a specificity of 92 %. The use of a direct millimeter method for the quantification of the carotid artery stenosis represents a very interesting option because it is possible to avoid cumbersome calculus and because the direct millimeter method overcomes the use of ratio-percent methods. Saba and Mallarini (2010b) confirmed the observations of Bartlett by showing that simple millimeter measurement of stenosis can reliably predict NASCET-type, ECST-type, and CSI-type percent stenosis.

### 13.3.5 Carotid Artery Plaque Characterization

It has been clearly demonstrated that diseased carotid arteries can contain large amounts of atherosclerotic mass without significant luminal narrowing due to compensatory outward remodeling of the artery (Toussaint et al. 1996). Thus, imaging methods that can reliably depict the lumen and the wall are needed to quantify the atherosclerotic plaque burden. For this reason it may be important to look beyond the degree of stenosis and try to determine plaque characteristics. By using CTA plaque has been differentiated into three categories, including fatty, mixed, and calcified lesions (Fig. 13.9), according to the Hounsfield unit (HU) measured in the plaque. In this classification, fatty (soft) plaques are those with a density value <50 HU, mixed plaques have density values between 50 and 119 HU, and

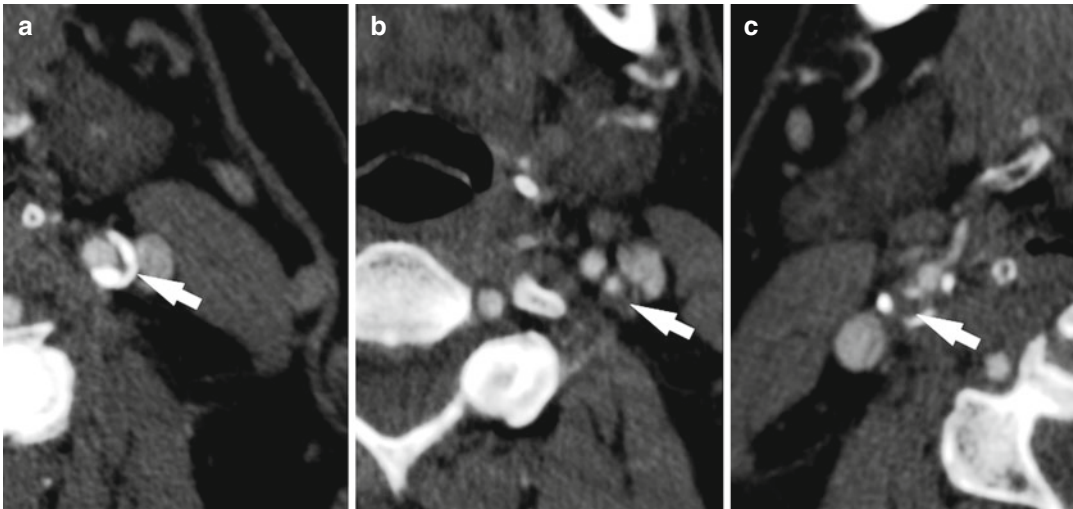


**Fig. 13.9** Different types of plaques according to HU values. CTA examples of calcified (a), mixed (b), and fatty (c) plaques, arrows indicate the plaque

calcified plaques have a density  $>120$  HU. It has been demonstrated that HU measurements in the center of fibrous-rich regions and lipid core are significantly different, and it has been suggested that very hypodense regions ( $<30$  HU) in the center of atherosclerotic carotid plaque are associated with the presence of a lipid core (e.g., lipid, hemorrhage, or necrotic debris). It is important to underline that fatty plaques at CTA are often associated with the presence of a lipid core, once thought to be an inert deposition of lipid, but now known to be a highly biologically active area. In carotid plaque analysis, two main parameters should be evaluated: morphology and composition. The plaque morphology can be classified into normal, irregular, or ulcerated (Fig. 13.10). Rothwell et al., by using DSA, demonstrated that irregular morphology is associated with the presence of cerebrovascular events (Rothwell et al. 2000). A plaque ulceration has been defined as “an intimal defect larger than  $1,000\ \mu\text{m}$  in width, exposing the necrotic core of the atheromatous plaque” (Saba et al. 2007b, c). It is important to identify this condition because ulcerated carotid plaques are associated with a higher risk of stroke or transient ischemic attack. Kim et al. (2000) demonstrated that the presence of ulceration alone is an important risk for neurological symptoms and a high-grade stenosis, combined with plaque ulceration, results in an increased risk of

stroke. The NASCET study showed that in the group of patients who received medical therapy, 30 % of the patients who had a severe carotid stenosis associated with an ulcerated plaque suffered an ischemic cerebral event within 2 years, while only 17 % of patients with severe stenosis but no ulcerated plaques had an ischemic cerebral event within 2 years (European Carotid Surgery Trialists’ Collaborative Group 1998). Among the imaging techniques, DSA was not sufficiently reliable for detecting ulcers in the carotid plaque (the sensitivity was 74 % and the specificity was 46 %) (Randoux et al. 2001; Walker et al. 2002), whereas MDCTA showed optimal results with a sensitivity of 93 % (Saba et al. 2007b); the presence of heavily calcified plaque limits CTA in the detection of ulcers (Schwartz et al. 1992; Cumming and Morrow 1994). Also, MRI showed good results in detecting plaque ulceration (Alvarez-Linera et al. 2003), whereas the results obtained by ultrasound are quite low, with a sensitivity of 38 %. When analyzing the plaque composition, two parameters should be identified: the fibrous cap and plaque characteristics.

The fibrous cap is a layer of fibrous connective tissue. It has been well demonstrated that a thin fibrous cap and its rupture are associated with the presence of strokes or transient ischemic attack. Saba and Mallarini (2009b), using CTA, showed that the presence of a fissured fibrous cap was

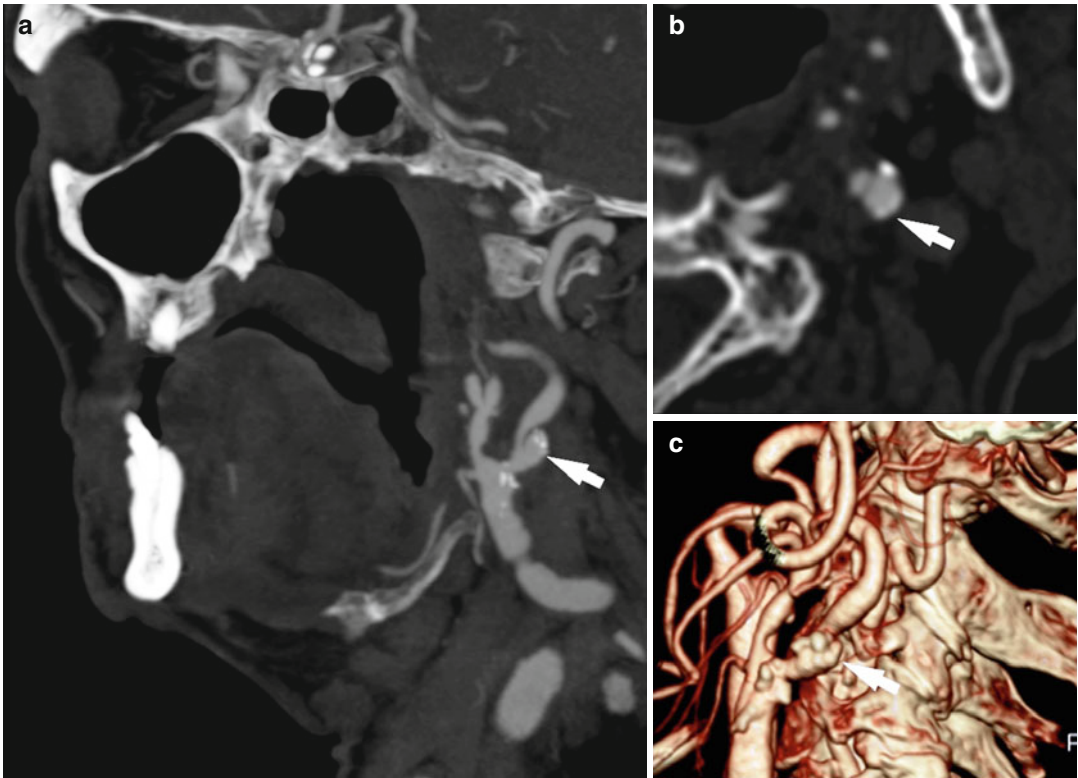


**Fig. 13.10** Ulcerated carotid artery plaque in a 65-year-old patient with left-sided stroke. Maximum-intensity projection (c, d), axial (b), and volume rendering (a) images show an ulcerated plaque in the left internal carotid artery, arrows indicate the ulcer

associated with cerebrovascular events ( $p=0.0032$ ). MRI is nowadays the best imaging technique to study the fibrous cap, its thickness, and its fissuration (Parker et al. 1991; Mitsumori et al. 2003; Kramer et al. 2004; Wasserman et al. 2002). In the literature it is quite well demonstrated that high-resolution MRI using blood- and fat-suppressed sequences (black-blood MRI) can well distinguish intact, thick fibrous caps from thin or ruptured fibrous caps. On MRI a thick fibrous cap appears as a juxtaluminal band of low signal in ToF images. In plaques with thin fibrous caps, this dark juxtaluminal band is absent. In plaques with a ruptured fibrous cap, the dark band is absent and there is a region of hyperintense signal adjacent to the lumen. Ultrasound showed suboptimal results in the study of the fibrous cap; Waki et al. (2003) demonstrated that ultrasound can distinguish between thin and thick fibrous caps in correlation with histology, but Sztajzelet et al. (2005), studying 31 plaques derived from

28 patients undergoing carotid endarterectomy, obtained a sensitivity and specificity of 73 and 67 %, respectively, in quantification of the thickness of the fibrous cap. The use of CT in assessing fibrous caps has not been studied extensively, and its sensitivity is still debatable. Saba and Mallarini (2009b) proposed CTA for the study of fissured fibrous caps, and Wintermark et al. (2008b, c; Arora et al. 2010) demonstrated that it is possible to measure fibrous cap thickness by using an automatic computer algorithm that quantitatively assesses the thickness of the fibrous cap, with significant results compared to histopathology ( $R^2=0.77$ ).

In the analysis of the plaque characteristics, the identification and quantification of calcium represents an important step because the presence of calcium in the carotid artery plaque seems to relate to a lower risk of cerebrovascular events (Nandalur et al. 2005, 2007; Saba et al. 2009; Hunt et al. 2002); in fact it is hypothesized that

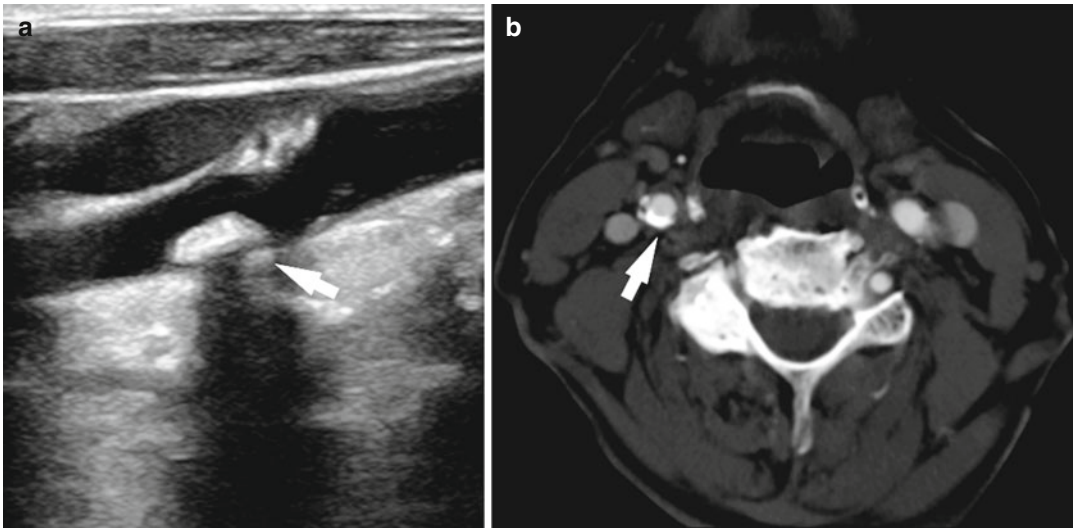


**Fig. 13.11** Calcified plaque (*arrows*). Examples of calcified plaque in ultrasound (**a**) and CT (**b**). In *panel a* the acoustic shadowing determined by the calcific components of the plaque is clearly visible, *arrows* indicate in both panels the calcified plaques

calcium may confer stability, resulting in protection against biomechanical stress. The presence of calcium in the carotid artery plaque can be evaluated by using CTA, MRA, or color Doppler echocardiography, but the most sensitive technique in detection, characterization, and quantification remains CTA because of the high coefficient of linear attenuation produced by CT calcium imaging (Fig. 13.11).

Another important plaque characteristic is intra-plaque hemorrhage. It is hypothesized that the extravasation of red blood cells or iron accumulation in plaque may represent plaque instability and promote plaque progression (Kolodgie et al. 2003). The mechanisms that lead to intra-plaque hemorrhage are still debated. In an old study by Patterson (1938), it was hypothesized that intra-plaque hemorrhage is secondary to the rupture of the vasa vasorum, but other authors suggested that the condition is due to cracks or fissures that may originate at the luminal surface (Davies and Thomas 1985; Constantinides 1966). It is interesting to observe that intra-plaque hemorrhages are more common in those carotid arteries that have a stenosis >70%. MRI is considered the best imaging technique to identify intra-plaque hemorrhage. In 2003 Moody and colleagues (2003) showed that

T1-weighted sequences are very sensitive in this kind of identification. Ultrasound is not very sensitive in the identification of hemorrhage; sometimes intra-plaque hemorrhage can be identified by the presence of a hypo-echogenic area within the plaque (Tahmasebpour et al. 2005). Whether it is possible to visualize intra-plaque hemorrhage with CTA is still debated. Recently, a paper by U-King-Im et al. (2010) showed that mean CT plaque density was higher for plaques with MRI-defined intraparenchymal hemorrhage (47 HU) compared with without intraparenchymal hemorrhage (43 HU;  $P=0.02$ ). Other authors showed that automated software classification may correctly detect intra-plaque hemorrhage (Wintermark et al. 2008d).

Another significant feature of carotid artery plaque is the presence or absence of thrombus. It is accepted that the presence of a plaque thrombus is a risk factor for the development of cerebrovascular events because the thrombus may determine the development of distal embolization. An association between plaque thrombus and ulcerated carotid plaque has been described (Rothwell et al. 2000). Even in this case the best imaging modality to study this condition is probably MRI which has the



potential to distinguish fresh thrombi from 1-week-old thrombi and occluding old thrombi (Funaki et al. 2011; Altaf et al. 2011).

---

## 13.4 Central Vessels

### 13.4.1 Aorta

In the past 15 years, great advancements have been made in the development of imaging procedures and techniques to explore thoracic and abdominal aortic pathology. In particular the development of MDCTA has led to shorter scanning times and higher spatial resolutions, this allowing a fast diagnosis of conditions like aneurysm rupture and arterial dissections. Nowadays, it is possible to quickly and accurately diagnose a wide range of traumatic and nontraumatic aortic conditions. For these reasons, nowadays, CTA is the preferred method for imaging in emergency abdominal vascular conditions because it enables the acquisition of high-spatial-resolution volumetric image data during a single-breath hold. The most frequent and severe conditions, in particular in elderly people, are abdominal aortic aneurysms and its rupture and aortic dissections.

#### 13.4.1.1 Abdominal Aortic Aneurysm

An arterial aneurysm is defined as a focal dilation of a blood vessel with respect to the original artery. Each year in the United States, abdominal aortic aneurysm (AAA) ruptures cause 4,500 deaths, with an additional 1,400 deaths resulting from the 45,000 repair procedures performed to prevent a rupture. Aneurysmal dilation of the aorta is present when there is a diameter of more than 32 mm in the case of thoracic aorta and 29 mm in the case of infrarenal abdominal aorta (Mewhort et al. 2011; Budde et al. 2011; Frauenfelder et al. 2004). Based on this criterion, the study authors reported that 9 % of all people older than 65 have an AAA (Alcorn et al. 1996; Baumgartner et al. 2008). It was reported that the 1-year incidence of AAA rupture according to initial diameter was 9.4 % for diameters of 5.5–5.9 cm, 10.2 % for diameters of 6.0–6.9 cm (19.1 % for the subgroup of 6.5–6.9 cm), and

32.5 % for diameters of 7.0 cm or more (Lederle et al. 2002; Conway et al. 2001; Reed et al. 1997). Approximately 80 % of aortic aneurysms occur between the aortic bifurcation and the renal arteries. Aortic aneurysms constitute the 14th leading cause of death in the United States. The decision to screen for AAA is difficult to make because it would expose many previously undiagnosed small aneurysms that are unlikely to rupture, resulting in needless disease labeling because only aneurysms of a certain size are considered for surgery, with smaller aneurysms subject to watchful waiting. In the past authors analyzed the effectiveness of population-based screening for AAA with abdominal ultrasound in people older than 65 years of age (Fleming et al. 2005) and concluded that a mortality reduction of approximately 50 % can be obtained by using ultrasound screening (Norman et al. 2004).

It is possible to detect and characterize AAA by using ultrasound, MR, and CT, but nowadays the best imaging modality to identify and characterize the presence of AAA is CTA. By using CTA it is possible to gather all necessary information to select the correct therapeutic approach. The introduction of MDCT technology allowed noninvasive imaging of the abdominal aorta (Fig. 13.12) and iliac arteries with improved spatial resolution and temporal resolution, thanks to the use of a thinner collimation. Moreover, CTA is commonly considered the standard of reference in the detection of endoleaks because of its noninvasive nature, widespread availability, and high sensitivity and specificity (Harris et al. 1999; Hittmair and Fleischmann 2001; Gorich et al. 2001). High-quality MDCTA can be obtained with the use of thin collimations (1–2 mm), which allow increased spatial resolution of both axial and 3D images.

MRI also showed good results in the detection and characterization of AAA (Kaufman et al. 1994; Weishaupt et al. 2000; Atar et al. 2006; Schwope et al. 2007), but this technique also has great potential to study the wall of the AAA by analyzing the uptake of the macrophage-specific contrast agent using ultra-small paramagnetic iron oxide (Truijers et al. 2009). The authors demonstrated that iron oxide uptake is limited or

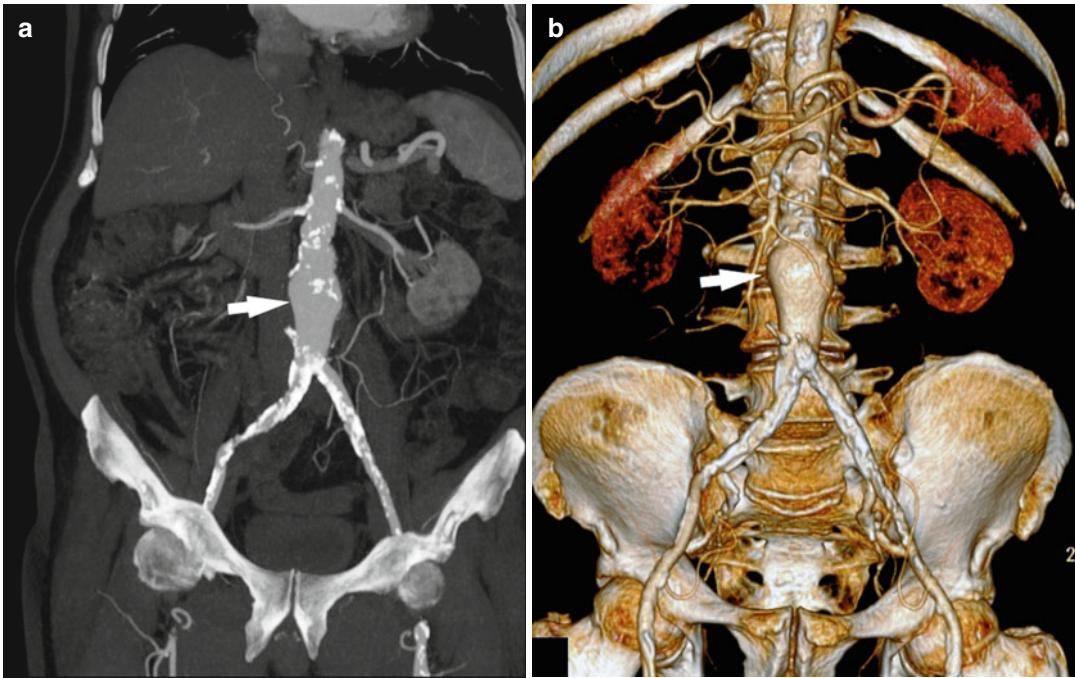


**Fig. 13.12** Abdominal aortic aneurysm. Maximum-intensity projection (a) and volume-rendered (b) post-processed CTA images show an abdominal aortic aneurysm (white arrow) in a 61-year-old patient

absent in the wall of normal-sized aortas and most aneurysms but individual abdominal aortic aneurysms exhibit high levels of uptake, indicative of extensive macrophage infiltration in the aneurysm wall.

It was found that aneurysm size is one of the strongest predictors of the risk of rupture (Aggarwal et al. 2011), with risk increasing markedly with aneurysm diameters greater than 5.5 cm; in fact the 5-year overall cumulative rupture rate of incidentally diagnosed AAA is 25–40 % for aneurysms larger than 5.0 cm, compared with 1–7 % for aneurysms 4.0–5.0 cm in diameter (Johansson et al. 1990; Nevitt et al. 1989). In the diagnosis of ruptured aneurysm, CTA is considered the gold standard mainly because it is possible to perform in emergency situations and obtain the results in a few minutes.

#### 13.4.1.2 Aortic Dissections

Aortic dissection is characterized by a spontaneous longitudinal separation of the aortic intima and adventitia caused by circulating blood

gaining access to and splitting the media of the aortic wall. This condition is the most common acute emergency condition of the aorta, often resulting in death. Each year, in the USA and Europe, there are 5,000 new cases of aortic dissection (Castañer et al. 2003; Hagan et al. 2000; Nienaber et al. 2004). The intimal tear, between intima and adventitial layers, allows blood to enter the media from the vessel lumen. The blood-filled space within the medial layer becomes a false lumen. This results in two lumina (the “true lumen” and the “false lumen”). The type and extent of the dissection as well as the presence of associated complications determine the overall outcome; therefore, evaluation of the entire aorta, branch vessels, and iliac and proximal femoral arteries is recommended to aid in treatment planning. In particular, assessment of the branch-vessel involvement and the relationship of the branch vessels to the true or the false lumen is extremely important because this kind of information aids in planning treatment with either root replacement, fenestration, or intravascular stent placement.

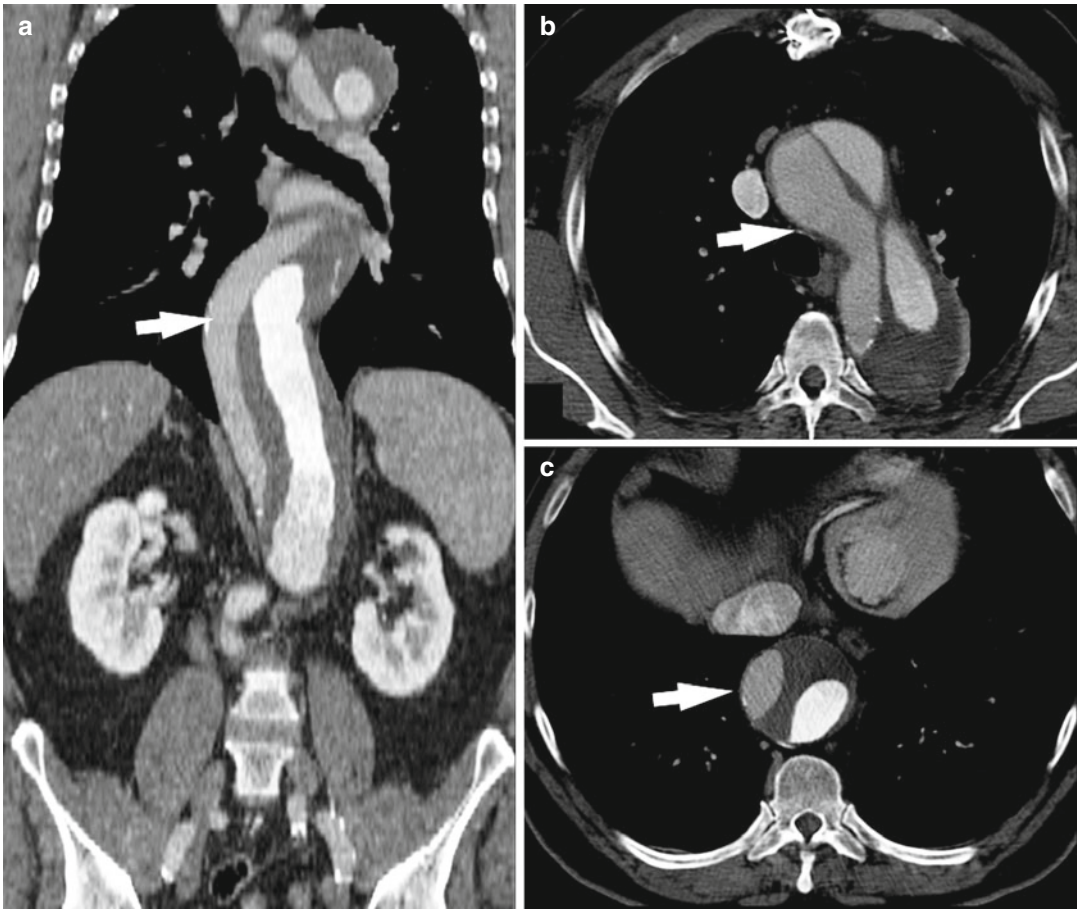


**Fig. 13.13** Aortic dissection. Multiplanar reconstruction (a) and axial images and (b, c) CTA images show an aortic dissection in a 43-year-old woman, arrows indicate the false lumen of the aneurysms

According to the temporal window, it is possible to distinguish acute and chronic dissections (Fig. 13.13). By definition, acute aortic dissections are characterized by symptoms that are present for less than 14 days; in chronic dissections the symptoms are present for 14 or more days.

The most used classification of the types of dissection is the Stanford classification, which is based on the need for surgical intervention. Stanford type A (60–70 % of all cases) refers to a dissection that involves the ascending thoracic aorta, and the dissection flap may extend into the descending aorta. Stanford type B refers to a dissection that involves the descending thoracic aorta distal to the left subclavian artery. Type A dissection is a more severe condition that typically requires urgent surgical intervention to

prevent extension into the aortic root, pericardium, or coronary arteries, whereas type B dissection is a less severe condition that usually requires only medical treatment.

Due to its wide availability and high diagnostic accuracy, MDCTA is the modality of choice for the evaluation of aortic dissection. With this technique it is possible to easily distinguish type A from type B dissection and localize the intimal entry site. When possible, ECG gating techniques (ECG triggering and retrospective ECG gating) should be used to minimize imaging artifacts caused by cardiac motion. With MDCTA it is quite easy to identify the intimal flap that occurs when blood enters the medial layer through an intimal tear, giving rise to a true lumen and a false lumen, with the flap separating the two lumina.

Sometimes, in chronic dissections with mural calcification of the false lumen, it is possible to observe a calcified false lumen. Authors have also reported an uncommon finding: the “Mercedes-Benz sign” when a three-channel dissection is present.

MRA is an accurate and noninvasive modality suitable for the investigation of aortic dissection in medically stable patients or those with chronic dissections, but it should not be used for patients whose condition is not stable. Like CTA, MRA can provide a complete visualization of the dissection by distinguishing the true lumen from the false lumen (Willmann et al. 2003; Hernández-Hoyos et al. 2002). MRA, compared to CTA, has the advantage of lacking ionizing radiation but suffers from the longer scan time required to perform the exam.

### 13.4.2 Pulmonary Arteries

Imaging of the pulmonary arteries requires fast imaging methods to avoid pulmonary artifacts from breathing. For these reasons, CTA is now the preferred method for imaging in pulmonary artery pathology, but things may change with new and promising advances in MRI. Several studies showed an increase in pulmonary artery pressures (namely, pulmonary hypertension) in elderly patients; another more prevalent condition is pulmonary embolism. In this section these two pathologies will be explored.

#### 13.4.2.1 Pulmonary Hypertension

Pulmonary hypertension identifies an increase in blood pressure in the pulmonary artery, pulmonary vein, or pulmonary capillaries. This condition is hemodynamically defined as a mean pulmonary artery pressure greater than 25 mmHg at rest or greater than 30 mmHg during exercise with an increased pulmonary vascular resistance (Grosse and Grosse 2010). Pulmonary hypertension can be a severe disease with a markedly decreased exercise tolerance and can result in heart failure. According to the most recent classification based on the etiology of the disease, it can be divided into five categories: arterial,

venous, hypoxic, thromboembolic, or miscellaneous (Simonneau et al. 2004).

Women are almost three times more likely to present with idiopathic pulmonary arterial hypertension than men. Up to 4 % of people who suffer a pulmonary embolism go on to develop chronic thromboembolic disease including pulmonary hypertension, and pulmonary venous hypertension occurs in most patients with congestive heart failure. In scleroderma the incidence of pulmonary hypertension has been estimated to be 6–60 % of all patients, in rheumatoid arthritis up to 21 %, and in systemic lupus erythematosus 4–14 %.

Usually, pulmonary arterial hypertension determines vasoconstriction of blood vessels. In addition, the increased workload of the heart causes hypertrophy of the right ventricle, making the heart less able to pump blood through the lungs, ultimately causing right heart failure. In pulmonary venous hypertension, there is no obstruction to blood flow in the lungs. Instead, the left heart fails to pump blood efficiently, leading to pooling of blood in the lungs. In chronic thromboembolic pulmonary hypertension, the blood vessels are blocked or narrowed with blood clots with increases in the blood pressure within the lungs which impairs the blood flow. In hypoxic pulmonary hypertension, the low levels of oxygen are thought to cause vasoconstriction or tightening of pulmonary arteries.

Because of the different pathways that can determine pulmonary hypertension, a series of tests must be performed to distinguish pulmonary arterial hypertension from venous, hypoxic, thromboembolic, or miscellaneous varieties.

Several papers have demonstrated the value of MDCT in the detection and characterization of pulmonary hypertension (Schwickert et al. 1994; Remy-Jardin et al. 1992, 2001; King et al. 1998). MDCT features of pulmonary hypertension can be classified as vascular or parenchymal changes (Grosse and Grosse 2010). Vascular changes include three different types of findings related to (1) pulmonary arterial hypertension (central pulmonary artery dilation, right heart chamber enlargement, atherosclerotic plaques), (2) chronic pulmonary thromboembolism (complete or partial thromboembolic obstruction, bands or webs



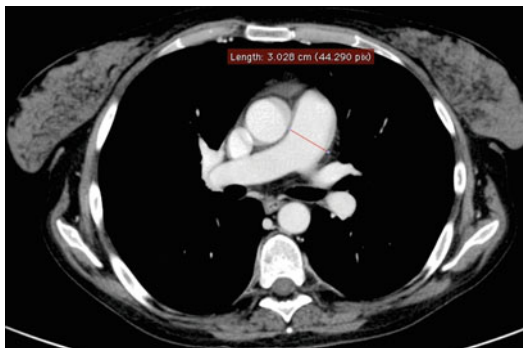


**Fig. 13.14** Pulmonary hypertension. CTA axial image in a 65-year-old patient with pulmonary hypertension. The diameter of the truncus of the pulmonary artery is 30 mm, demonstrating an enlargement of the structure

in the pulmonary arteries), and (3) systemic collateral supply. Parenchymal changes include mosaic lung perfusion and the presence of peripheral parenchymal opacities. In several studies in the late 1970s and early 1980s, investigators measured the diameter of central pulmonary arteries using CT findings to predict the presence of pulmonary hypertension (Fig. 13.14). Recently, some authors showed the value of dual-energy CTA in the study of pulmonary hypertension. Dual-energy CTA can provide high-spatial-resolution images of pulmonary vascular and parenchymal anatomy in combination with functional information on the pulmonary microcirculation from the same data set (Remy-Jardin and Remy 2008; Nakazawa et al. 2011). Results of a few studies in the late 1990s suggested the utility of velocity-encoded MRI with phase-contrast techniques as a noninvasive method for assessment of pulmonary hypertension, but the technique was not considered reliable. Improved MRI sequences and advances in gradient systems have made possible new 3D gradient-recalled echo sequences with ultra-short TR/TE that allow assessment of qualitative regional perfusion differences in the entire lung with high temporal resolution.

### 13.4.2.2 Pulmonary Embolism

Pulmonary embolism (PE) is a potentially life-threatening condition and is responsible for significant morbidity and mortality in adults (Ritchie et al. 2007; Tapson 2008). CTA is increasingly used

as a reliable, noninvasive first-line imaging study in both pediatric and adult patients with clinically suspected PE. Each year it is estimated that there are 600,000 episodes of PE in the United States with an overall mortality rate among untreated patients approaching 20–35 %: more than 80 % of deaths from PE occur in the first 30 min and 90 % within 2.5 h of the event (Righini et al. 2008; Stein et al. 1995; Calder et al. 2005). Two of the most widely used scoring systems are the Wells score and the Geneva clinical probability score (Wells et al. 1998; Le Gal et al. 2006; Wong et al. 2011). The Wells score is a clinical prediction rule, where the following parameters are considered: (a) clinically suspected deep venous thrombosis (DVT), 3.0 points; (b) alternative diagnosis is less likely than PE, 3.0 points; (c) tachycardia, 1.5 points; (d) immobilization/surgery in previous 4 weeks, 1.5 points; (e) history of DVT or PE, 1.5 points; (f) hemoptysis, 1.0 points; and (g) malignancy (treatment within 6 months, palliative), 1.0 points.

Among imaging techniques, it is possible to use different approaches. X-rays are often obtained of patients with shortness of breath to help rule out other causes, such as congestive heart failure and rib fracture. Chest X-rays are not sensitive or specific for PE and usually lack signs that suggest the diagnosis of PE (e.g., Hampton's hump, Westermark sign).

Ultrasound can offer indirect sign of pulmonary embolism by examining the legs in search of DVT. The presence of DVT, as shown on ultrasonography of the legs, according to some authors, is in itself enough to warrant anticoagulation, without requiring CTA. This may be a valid approach in pregnancy, in which other modalities, which use ionizing radiation, could increase the risk to the unborn child.

In the past years, the gold standard for diagnosing PE was pulmonary angiography. Pulmonary angiography nowadays is used less often due to wider acceptance of CTA, which is currently the recommended first-line diagnostic imaging test in most people.

Several studies (Remy-Jardin et al. 1996; Christiansen 1997; Mayo et al. 1997; Ghaye et al. 2002; Coche et al. 2003; Reinartz et al. 2004) have yielded data ascribing a high sensitivity and

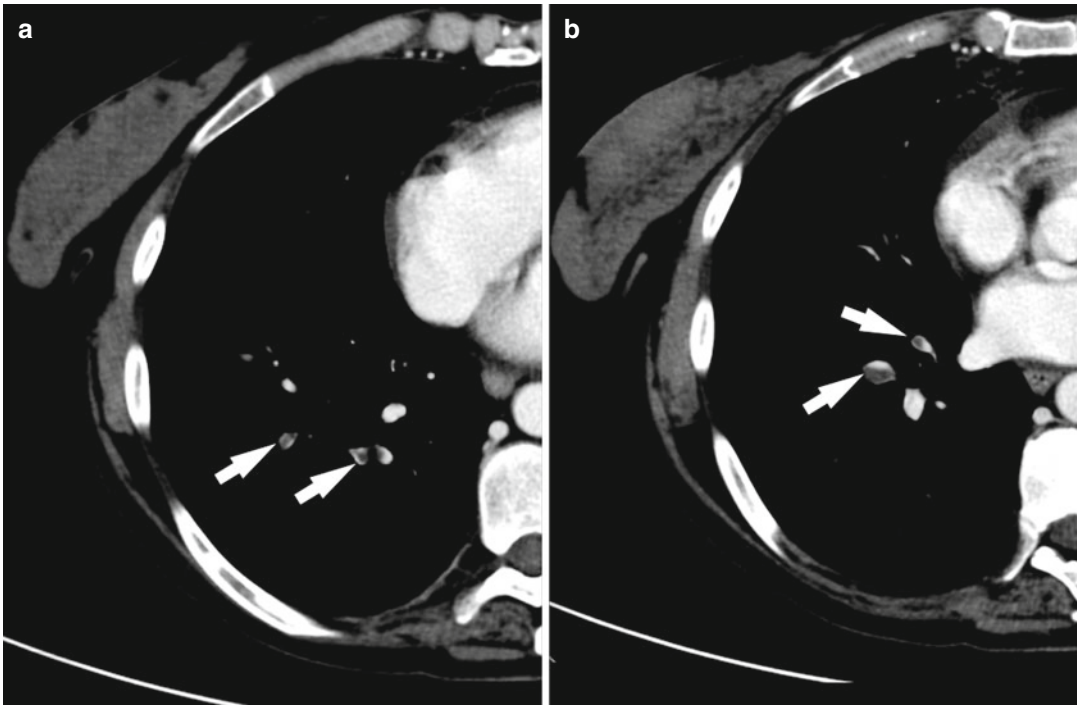


**Fig. 13.15** Pulmonary embolism. CTA axial images in a 58-year-old patient with pulmonary embolism (a, b). Multiple emboli are visible (*white arrows*)

specificity to CTA (Fig. 13.15) and showing acceptable clinical outcome among patients with normal findings on CTA. CTA is fast, easy, reliable, diagnostic, and widely available. These attributes have led to a significant increase in the number of patients undergoing imaging for PE since the late 1990s. CTA can show presence of intraluminal thrombus even in the more distal pulmonary arteries. Moreover, compared to DSA and MRA, CTA can offer important information regarding the parenchyma. This is important for planning the correct therapeutic approach.

## 13.5 Peripheral Vessels

The availability of state-of-the-art technology in ultrasound, CT, and MR revolutionized the evaluation of peripheral vasculature in atherosclerosis burden assessment and in those patients with vascular trauma. Evaluation of peripheral vasculature is an integral part of the management of

patients with peripheral vascular disease and in polytrauma patients with suspected vascular injury. In past years DSA was considered the gold standard in the evaluation of peripheral vessels, especially peripheral vascular disease, but nowadays the role of DSA has been challenged by recent advances in technology like ultrasound, CT, and MR. In particular CTA has experienced a technological quantum leap with the introduction of multiple detectors with isotropic imaging capabilities.

### 13.5.1 Lower Extremities

The most frequent cause of peripheral vascular disease in the lower extremities is atherosclerotic disease. Other causes of peripheral vascular disease like vascular aneurysms, cystic adventitial disease, or popliteal entrapment syndrome are less frequently detected (Fig. 13.16). Approximately eight million Americans are affected by peripheral arterial disease (Hirsch et al. 2001), and the

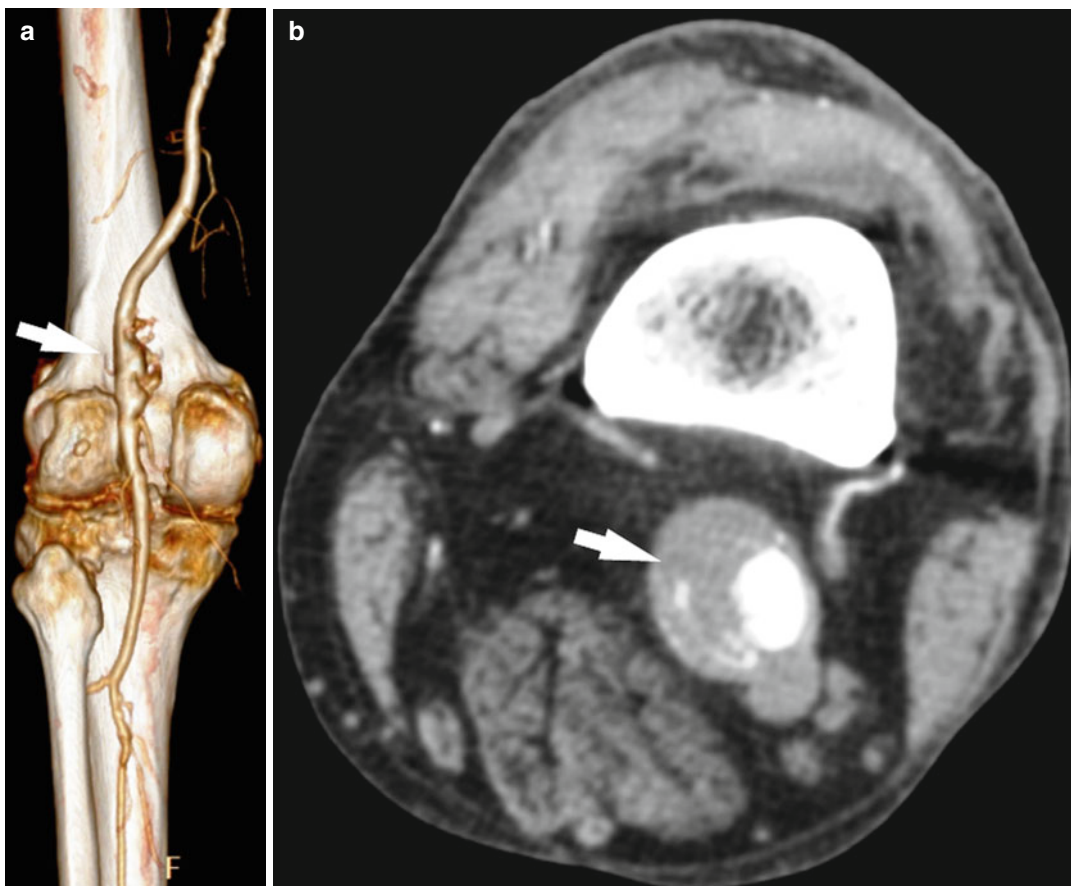


**Fig. 13.16** Popliteal artery aneurysm. 64-year-old patient with an aneurysm in the popliteal artery. Volume-rendered post-processed image (a) and CTA axial (b) image clearly demonstrate the presence of the aneurysm (white arrow)

estimated prevalence of this pathology in people older than 70 years is between 14 and 29 % (Selvin and Erlinger 2004). Intermittent claudication, the classical peripheral arterial disease symptom, is present in only 10 % of patients (Arain and Cooper 2008). It was reported that approximately 50 % of patients with peripheral arterial disease have atypical lower-extremity symptoms and another 40 % are asymptomatic. This heterogeneity of clinical presentations may explain why peripheral arterial disease is diagnosed and treated in only 25 % of affected patients. Patients with peripheral vascular disease may present with an acute limb threatening event, a chronic threatened limb, or merely claudication. Sometimes the disease site of greatest severity can be identified by the location of the patient's symptoms.

The purpose of imaging in the analysis of vascular disease of lower extremities is to detect the site and anatomical extent of obstruction, to delineate the presence or absence of significant obstruction to blood flow, and to assess the status of collateral flow and distal vasculature, for planning treatment as well as to monitor the results of therapy and disease progression (Lawrence et al. 1995; Rubin et al. 1999).

Ultrasonography is considered the initial imaging modality of choice in suspected peripheral vascular disease, especially in popliteal disease. This simple, cheap, and noninvasive test is very useful, but limitations reduce its potential. First, it is operator dependent and the interobserver agreement reported in some studies is quite poor. Second, ultrasound is unable to assess distal vasculature and fails to demonstrate direct

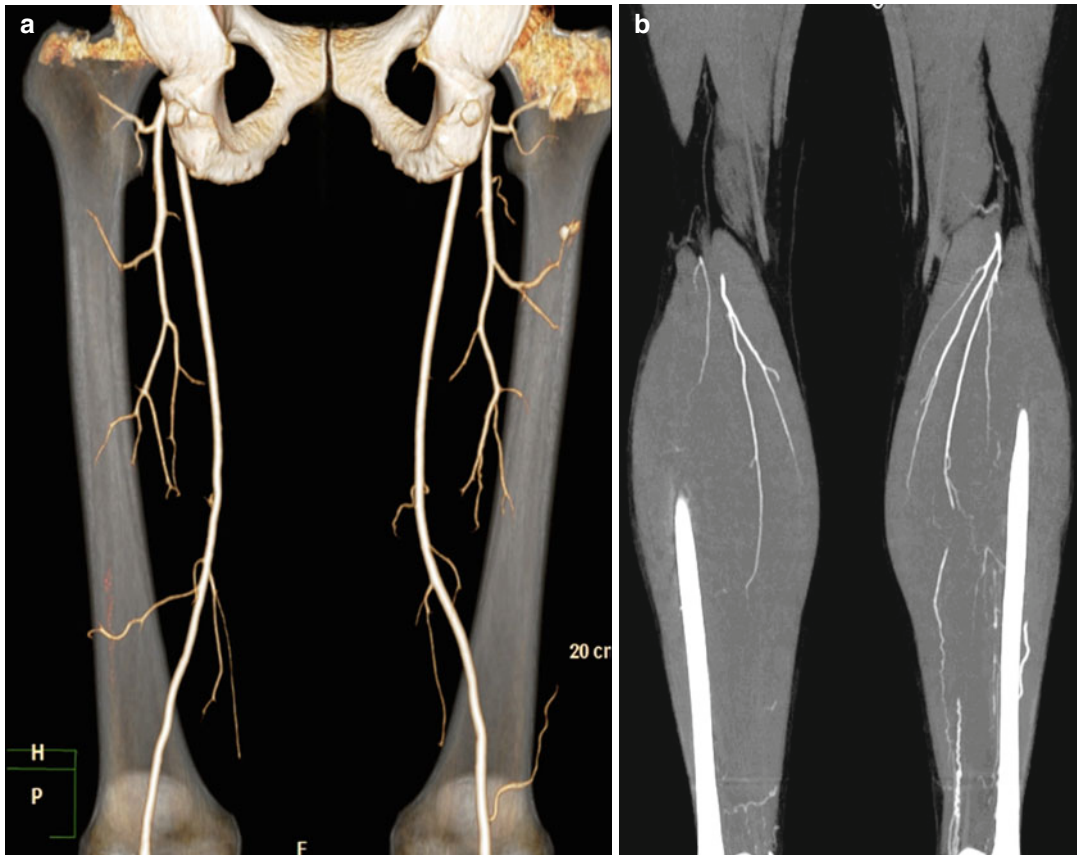


**Fig. 13.17** Atherosclerotic disease of the lower extremities. Volume-rendered (a) and maximum-intensity projection (b) post-processed CTA images show lower-extremity vasculature

evidence of cystic adventitial or popliteal entrapment syndrome. One of the most common ultrasound Doppler analyses is the ankle-brachial index (ABI). An abnormal ABI suggests a diagnosis of peripheral vascular disease. This test can quantify the severity of peripheral vascular disease and also predict the risk of future cardiovascular events. By using ultrasound, systolic blood pressures in the bilateral brachial, dorsalis pedis, and posterior tibial arteries are measured. The higher of two brachial artery systolic pressure measurements is used as the denominator. The right and left ABI values are determined by dividing the higher value of dorsalis pedis or posterior tibial pressure measurements in each leg by the brachial artery pressure. Usually, patients with claudication have ABI values ranging from 0.5 to 0.9.

Authors have reported that CTA has more than 92 % sensitivity, 96.2 % specificity, and an overall accuracy of more than 95.5 % in the evaluation of peripheral vascular disease (Joshi et al. 2004). (Fig. 13.17) One of the advantages of CTA is the detection and characterization of atherosclerotic plaques and the presence or absence of calcification within it. However, the presence of very heavy calcification is a disadvantage for CTA, as the vessels are then not adequately evaluated due to volume averaging artifacts, especially in vessels of smaller caliber, beyond the level of the inguinal ligament. The additional benefit of cross-sectional CT in simultaneously depicting extra-luminal structures causing arterial obstruction, as in popliteal artery entrapment or cystic adventitial disease, cannot be overemphasized. To avoid multiple acquisitions and



minimize radiation exposure and contrast medium volume, it is important to have fundamental knowledge of how to select the CT scan parameters. It is also important to know how to apply advanced workstation visualization techniques and tool functions for the lower-extremity vascular tree.

In the analysis of the vascular system of the lower extremities, probably the main limitation of CTA is the absence of any hemodynamic assessment, which can be obtained by Doppler imaging and MRA. However, compared to ultrasound, CTA is less operator dependent and it is clearly advantageous in patients with trauma who are often immobilized and in intense pain. Moreover, surgeons prefer CTA images to ultrasound as they are presented in a format similar to conventional angiograms with which they are more familiar and comfortable.

Another frequently used technique for the study of peripheral vascular disease is MRA. Compared to CTA, MRA has the advantage of being unaffected by the presence of vascular calcification and, given excellent results, in the evaluation of the distal anterior tibial, peroneal, and dorsalis pedis arteries. Recently, Kos et al. (2009) showed that Gadofosveset-enhanced MRA of the pedal arteries in patients with peripheral arterial occlusive disease has arterial visibility equal to DSA and that it facilitates depiction of clinically significant stenosis and occlusion. Other authors assessed the potential of MRI for popliteal entrapment (Ozkan et al. 2008). They found that MRI allows visualization of an abnormal relationship of the popliteal artery to adjacent musculotendinous structures, and it can demonstrate more than one abnormality. However, MRI is contraindicated by implanted devices such as pacemakers, defibrillators, and metal aneurysm clips. Moreover, gadolinium, the contrast agent used for MRA scans, recently has been linked to development of nephrogenic systemic fibrosis in patients with a glomerular filtration rate of less than 30 mL/min or those receiving long-term dialysis (Sadowski et al. 2007).

### 13.5.2 Upper Extremities

From a technical and interpretative perspective, vascular imaging applications in the

upper extremities are challenging. Aging has marked effects on the cardiovascular system in many ways. Nevertheless, it can be difficult to separate the effect of true normal vascular aging from disease-related changes in Western populations. Cross-sectional studies have shown an age-related increase in arterial diameter, length, and wall thickness of the brachial artery. Although vascular disorders of the upper extremity are less common than in the lower extremities, they may carry a poorer prognosis. The most common vascular pathologies involving the upper extremities are vascular injuries, arterial occlusion, arterial extravasation, vasculitis, focal stenosis, and pseudoaneurysm (Anderson et al. 2008; Pieroni et al. 2009; Foster et al. 2011). An important and interesting modern application of imaging is to explore the upper-extremity vessels in patients who have undergone plastic surgery (Audolfsson et al. 2009; Balakrishnan 2011).

It is possible to image pathologies affecting the upper extremities by using ultrasound, CT, and MR, but usually CT and MR are used. Ultrasound is commonly used as “first-line” exam for the analysis of the upper extremities, but it is too operator dependent.

Given the improved temporal resolution using modern MDCT technology, with the ability to acquire isotropic data sets and the myriad post-processing options, upper-extremity arterial visualization and characterization is now common (Fig. 13.18). Moreover, the replacement of DSA with CTA for extremity trauma reflects practice that is common for the lower extremities, given decreased morbidity associated with CT and the excellent image quality provided by current MD-CT technology. However, obtaining an optimal analysis of the arteries of the upper extremities can be difficult by using CTA because synchronizing the relatively large scan coverage with a single bolus of contrast medium requires precise selection of acquisition and contrast delivery parameters. Evaluation of upper-extremity trauma poses considerable additional technical challenges, including the smaller size of the arterial bed and difficulties in proper positioning during image acquisition.



**Fig. 13.18** Disease of the upper extremities. Volume-rendered (a) and maximum-intensity projection (b) post-processed CTA images show right-arm vasculature of a patient with neurofibromatosis

Authors have demonstrated that MRI accurately defines steno-occlusive lesions in patients with atherosclerosis and embolus; moreover, it can help to diagnose thoracic outlet syndrome, vascular malformations, and vasculitis. Some studies have shown that MRI can identify vascular injuries after blunt or occupational trauma, corkscrew collaterals in Burger disease, and pathological vessels in malignant tumors and have suggested that this

technique can be used for planning the treatment of vascular disorders of the upper extremities (Razek et al. 2010).

### Conclusions

Nowadays, the use of advanced imaging technologies allows exploration of peripheral vascular pathology with an exquisite level of detail. The most important methodologies today are ultrasound, CT, and MRI.

Usually ultrasound represents a “first-line” exam and it is possible to obtain good diagnostic results; however, it suffers two main limitations: the first is the poor interobserver variability. The second one is the presence of some physical limitations that reduce the applicability and diagnostic accuracy of the technique (e.g., presence of calcium in the vessels, uncooperative patients). These two limits do not allow the use of ultrasound for advanced vascular disease characterization.

CT and MR are both “second-line” exams and they can explore the entire vascular system. CT is probably used more to explore the peripheral arterial system and offers a better level of detail than MRI. Still, MRI has two main advantages compared to CTA: no radiation exposure and, in some cases, no need for contrast material.

## References

- Aggarwal S, Qamar A, Sharma V, Sharma A (2011) Abdominal aortic aneurysm: a comprehensive review. *Exp Clin Cardiol* 16(1):11–15
- Alcorn HG, Wolfson SK, Sutton-Tyrrell K, Kuller LH, O’Leary D (1996) Risk factors for abdominal aortic aneurysms in older adults enrolled in The Cardiovascular Health Study. *Arterioscler Thromb Vasc Biol* 16(8):963–970
- Altaf N, Goode SD, Beech A, Gladman JR, Morgan PS, MacSweeney ST, Auer DP (2011) Plaque hemorrhage is a marker of thromboembolic activity in patients with symptomatic carotid disease. *Radiology* 258(2):538–545
- Alvarez O, Edwards JH, Hyman RA (1986) MR recognition of internal carotid artery occlusion. *AJNR Am J Neuroradiol* 7:359–360
- Alvarez-Linera J, Benito-Leon J, Escribano J, Campollo J, Gesto R (2003) Prospective evaluation of carotid artery stenosis: elliptic centric contrast-enhanced MR angiography and spiral CT angiography compared with digital subtraction angiography. *AJNR Am J Neuroradiol* 24:1012–1019
- Anderson SW, Foster BR, Soto JA (2008) Upper extremity CT angiography in penetrating trauma: use of 64-section multidetector CT. *Radiology* 249(3):1064–1073
- Anidjar S, Salzmann JL, Gentric D, Lagneau P, Camilleri JP, Michel JB (1990) Elastase-induced experimental aneurysms in rats. *Circulation* 82:973–981
- Araín FA, Cooper LT (2008) Peripheral arterial disease: diagnosis and management. *Mayo Clin Proc* 83(8):944–949
- Arora S, Chien JD, Cheng SC, Chun KA, Wintermark M (2010) Optimal carotid artery coverage for carotid plaque CT-imaging in predicting ischemic stroke. *J Neuroradiol* 37(2):98–103
- Atar E, Belenky A, Hadad M, Ranany E, Baytner S, Bachar GN (2006) MR angiography for abdominal and thoracic aortic aneurysms: assessment before endovascular repair in patients with impaired renal function. *AJR Am J Roentgenol* 186(2):386–393
- Audolfsson T, Rozen WM, Wagstaff MJ, Whitaker IS, Acosta R (2009) A reliable and aesthetic technique for cephalic vein harvest in DIEP flap surgery. *J Reconstr Microsurg* 25(5):319–321
- Balakrishnan G (2011) Vascular anomalies of the upper limb. *Indian J Plast Surg* 44(2):276–282
- Bartlett ES, Walters TD, Symons SP, Fox AJ (2006a) Quantification of carotid stenosis on CT angiography. *AJNR Am J Neuroradiol* 27:13–19
- Bartlett ES, Symons SP, Fox AJ (2006b) Correlation of carotid stenosis diameter and cross-sectional areas with CT angiography. *AJNR Am J Neuroradiol* 27:638–642
- Bartlett ES, Walters TD, Symons SP, Fox AJ (2007) Carotid stenosis index revised with direct CT angiography measurement of carotid arteries to quantify carotid stenosis. *Stroke* 38:286–291
- Baumgartner I, Hirsch AT, Abola MT, Cacoub PP, Poldermans D, Steg PG, Creager MA, Bhatt DL (2008) Cardiovascular risk profile and outcome of patients with abdominal aortic aneurysm in outpatients with atherothrombosis: data from the Reduction of Atherothrombosis for Continued Health (REACH) Registry. *J Vasc Surg* 48(4):808–814
- Briley-Saebo KC, Mulder WJ, Mani V (2007) Magnetic resonance imaging of vulnerable atherosclerotic plaques: current imaging strategies and molecular imaging probes. *J Magn Reson Imaging* 27:460–479
- Budde RP, Kluin J, van Herwerden LA, Prokop M (2011) Comprehensive dynamic aortic and cardiac analysis by 256-slice computed tomography in type A dissection. *Ann Thorac Surg* 92(3):e47–e48
- Butler J, Kalogeropoulos AP, Georgiopoulou VV, Bibbins-Domingo K, Najjar SS, Sutton-Tyrrell KC, Harris TB, Kritchevsky SB, Lloyd-Jones DM, Newman AB, Psaty BM (2011) Systolic blood pressure and incident heart failure in the elderly. The Cardiovascular Health Study and the Health, Ageing and Body Composition Study. *Heart* 97(16):1304–1311
- Calder KK, Herbert M, Henderson SO (2005) The mortality of untreated pulmonary embolism in emergency department patients. *Ann Emerg Med* 45(3):302–310
- Calhoun PS, Kuszyk BS, Heath DG, Carley JC, Fishman EK (1999) Three-dimensional volume rendering of spiral CT data: theory and method. *Radiographics* 19:745–764
- Casscells W, Naghavi M, Willerson JT (2003) Vulnerable atherosclerotic plaque: a multifocal disease. *Circulation* 107(16):2072–2075
- Castañer E, Andreu M, Gallardo X, Mata JM, Cabezuolo MA, Pallardó Y (2003) CT in nontraumatic acute thoracic aortic disease: typical and atypical features and complications. *Radiographics* 23(Spec No 4):S93–110

- Choudhury RP, Fuster V, Badimon JJ, Fisher EA, Fayad ZA (2002) MRI and characterization of atherosclerotic plaque: emerging applications and molecular imaging. *Arterioscler Thromb Vasc Biol* 22(7): 1065–1074
- Christiansen F (1997) Diagnostic imaging of acute pulmonary embolism. *Acta Radiol Suppl* 410:1–33
- Cliff WJ (1970) The aortic tunica media in aging rats. *Exp Mol Pathol* 13:172–189
- Coche E, Verschuren F, Keyeux A, Goffette P, Goncette L, Hainaut P, Hammer F, Lavenne E, Zech F, Meert P, Reynaert MS (2003) Diagnosis of acute pulmonary embolism in outpatients: comparison of thin-collimation multi-detector row spiral CT and planar ventilation-perfusion scintigraphy. *Radiology* 229(3): 757–765
- Constantinides P (1966) Plaque fissuring in human coronary thrombosis. *J Atheroscler Res* 6:1–17
- Conway KP, Byrne J, Townsend M, Lane IF (2001) Prognosis of patients turned down for conventional abdominal aortic aneurysm repair in the endovascular and sonographic era: Szilagyi revisited? *J Vasc Surg* 33:752–757
- Cumming MJ, Morrow IA (1994) Carotid artery stenosis: a prospective comparison of CT angiography and conventional angiography. *AJR Am J Roentgenol* 163: 517–523
- Davies MJ, Thomas AC (1985) Plaque fissuring: the cause of acute myocardial infarction, sudden ischaemic death, and crescendo angina. *Br Heart J* 53:363–373
- Dawson DL, Zierler RE, Strandness DE (1993) The role of duplex scanning and arteriography before carotid endarterectomy: a prospective study. *J Vasc Surg* 18: 673–680
- Eliasziv M, Rankin RN, Fox AJ (1995) Accuracy and prognostic consequences of ultrasonography in identifying severe carotid artery stenosis. *Stroke* 26: 1747–1752
- European Carotid Surgery Trialists' Collaborative Group (1998) Randomised trial of endarterectomy for recently symptomatic carotid stenosis: final results of the MRC European Carotid Surgery Trial (ECST). *Lancet* 351:1379–1387
- Executive Committee for the Asymptomatic Carotid Atherosclerosis Study (1995) Endarterectomy for asymptomatic carotid artery stenosis. *JAMA* 273: 1421–1428
- Fishman E (2003) A brief overview of CT angiography. *Appl Radiol* 32:9–11
- Fleming C, Whitlock EP, Beil TL et al (2005) Screening for abdominal aortic aneurysm: a best-evidence systematic review for the US Preventive Services Task Force. *Ann Intern Med* 142:203–211
- Fornieri C, Quaglino D, Mori G (1992) Role of the extracellular matrix in age-related modifications of the rat aorta. Ultrastructural, morphometric and enzymatic evaluations. *Arterioscler Thromb* 12:1008–1016
- Foster BR, Anderson SW, Uyeda JW, Brooks JG, Soto JA (2011) Integration of 64-detector lower extremity CT angiography into whole-body trauma imaging: feasibility and early experience. *Radiology* 261(3): 787–795
- Frauenfelder T, Wildermuth S, Marincek B, Boehm T (2004) Nontraumatic emergent abdominal vascular conditions: advantages of multi-detector row CT and three-dimensional imaging. *Radiographics* 24(2): 481–496
- Funaki T, Iihara K, Miyamoto S, Nagatsuka K, Hishikawa T, Ishibashi-Ueda H (2011) Histologic characterization of mobile and nonmobile carotid plaques detected with ultrasound imaging. *J Vasc Surg* 53(4):977–983
- Fuster V, Stein B, Ambrose JA, Badimon L, Badimon JJ, Chesebro JH (1990) Atherosclerotic plaque rupture and thrombosis: evolving concepts. *Circulation* 82(Suppl 3):II47–II59
- Gao T, Zhang Z, Yu W, Zhang Z, Wang Y (2009) Atherosclerotic carotid vulnerable plaque and subsequent stroke: a high-resolution MRI study. *Cerebrovasc Dis* 27(4):345–352
- Gerrity RG, Cliff WF (1972) The aortic tunica intima in young and aging rats. *Exp Mol Pathol* 16:382–402
- Ghaye B, Remy J, Remy-Jardin M (2002) Non-traumatic thoracic emergencies: CT diagnosis of acute pulmonary embolism: the first 10 years. *Eur Radiol* 12(8): 1886–1905
- Goodson SF, Flanagan P, Bishara RA (1987) Can carotid duplex scanning supplant arteriography in patients with focal carotid territory symptoms? *J Vasc Surg* 5:551–557
- Gorich J, Rilinger N, Sokiranski R et al (2001) Endoleaks after endovascular repair of aortic aneurysm: are they predictable? Initial results. *Radiology* 218:477–480
- Grosse C, Grosse A (2010) CT findings in diseases associated with pulmonary hypertension: a current review. *Radiographics* 30(7):1753–1777
- Guagliumi G, Sirbu V (2008) Optical coherence tomography: high resolution intravascular imaging to evaluate vascular healing after coronary stenting. *Catheter Cardiovasc Interv* 72(2):237–247
- Guagliumi G, Musumeci G, Sirbu V, Bezerra HG, Suzuki N, Fiocca L, Matiashvili A, Lortkipanidze N, Trivisonno A, Valsecchi O, Biondi-Zoccai G, Costa MA (2010) Optical coherence tomography assessment of in vivo vascular response after implantation of overlapping bare-metal and drug-eluting stents. *JACC Cardiovasc Interv* 3(5):531–539
- Guyton JR, Lindsay KL, Dao DT (1983) Comparison of aortic intima and inner media in young adult versus aging rats. *Am J Pathol* 111:234–246
- Hagan PG, Nienaber CA, Isselbacher EM, Bruckman D, Karavite DJ, Russman PL, Evangelista A, Fattori R, Suzuki T, Oh JK, Moore AG, Malouf JF, Pape LA, Gaca C, Sechtem U, Lenferink S, Deutsch HJ, Diedrichs H, Marcovsky J, Llovet A, Gilon D, Das SK, Armstrong WF, Deeb GM, Eagle KA (2000) The International Registry of Acute Aortic Dissection (IRAD): new insights into an old disease. *JAMA* 283(7):897–903



- Hardie AD, Kramer CM, Raghavan P (2007) The impact of expansive arterial remodelling on clinical presentation in carotid artery disease: a multi-detector-row CT angiography study. *AJNR Am J Neuroradiol* 28:1067–1070
- Harris P, Brennan J, Martin J et al (1999) Longitudinal aneurysm shrinkage following endovascular aortic aneurysm repair: a source of intermediate and late complications. *J Endovasc Surg* 6:11–16
- Haudenschild CC, Prescott MF, Chobanian AV (1981) Aortic endothelial and subendothelial cells in experimental hypertension and aging. *Hypertension* 3(Suppl 1): 148–153
- Hernández-Hoyos M, Orkisz M, Puech P, Mansard-Desbleds C, Douek P, Magnin IE (2002) Computer-assisted analysis of three-dimensional MR angiograms. *Radiographics* 22(2):421–436
- Hirsch AT, Criqui MH, Treat-Jacobson D et al (2001) Peripheral arterial disease detection, awareness, and treatment in primary care. *JAMA* 286(11):1317–1324
- Hittmair K, Fleischmann D (2001) Accuracy of predicting and controlling time-dependent aortic enhancement from a test bolus injection. *J Comput Assist Tomogr* 25:287–294
- Hunt JL, Fairman R, Mitchell ME, Carpenter JP, Golden M, Khalapyan T, Wolfe M, Neschis D, Milner R, Scoll B, Cusak A, Moheler ER (2002) Bone formation in carotid plaques. A clinicopathological study. *Stroke* 33:1214–1219
- Jaff MR, Goldmakher GV, Lev MH, Romero JM (2008) Imaging of the carotid arteries: the role of duplex ultrasonography, magnetic resonance arteriography, and computerized tomographic arteriography. *Vasc Med* 13:281–292
- Jefferson AL, Himali JJ, Au R, Seshadri S, Decarli C, O'Donnell CJ, Wolf PA, Manning WJ, Beiser AS, Benjamin EJ (2011) Relation of left ventricular ejection fraction to cognitive aging (from the Framingham Heart study). *Am J Cardiol* 108(9):1346–1351
- Johansson G, Nydahl S, Olofsson P et al (1990) Survival in patients with abdominal aortic aneurysms. Comparison between operative and nonoperative management. *Eur J Vasc Surg* 4:497–502
- Joshi A, Nimbkar V, Merchant S, Mhashelkar Y, Talekar K (2004) Role of CT angiography in the evaluation of peripheral vasculature using MSCT – our initial experience. *Indian J Radiol Imaging* 14:309–315
- Kaufman JA, Geller SC, Petersen MJ, Cambria RP, Prince MR, Waltman AC (1994) MR imaging (including MR angiography) of abdominal aortic aneurysms: comparison with conventional angiography. *AJR Am J Roentgenol* 163(1):203–210
- Kim DI, Lee SJ, Lee BB, Kim YI, Chung CS, Seo DW, Lee KH, Ko YH, Kim DK, Do YS, Byun HS (2000) The relationship between the angiographic findings and the clinical features of carotid artery plaque. *Surg Today* 30:37–42
- King MA, Ysrael M, Bergin CJ (1998) Chronic thromboembolic pulmonary hypertension: CT findings. *AJR Am J Roentgenol* 170(4):955–960
- Kolodgie FD, Gold HK, Burke AP et al (2003) Intraplaque hemorrhage and progression of coronary atheroma. *N Engl J Med* 349:2316–2325
- Kolodgie FD, Nakazawa G, Sangiorgi G, Ladich E, Burke AP, Virmani R (2007) Pathology of atherosclerosis and stenting. *Neuroimaging Clin N Am* 17(3): 285–301
- Kos S, Reisinger C, Aschwanden M, Bongartz GM, Jacob AL, Bilecen D (2009) Pedal angiography in peripheral arterial occlusive disease: first-pass i.v. contrast-enhanced MR angiography with blood pool contrast medium versus intraarterial digital subtraction angiography. *AJR Am J Roentgenol* 192(3):775–784
- Kramer CM, Cerilli LA, Hagspiel K, DiMaria JM, Epstein FH, Kern JA (2004) Magnetic resonance imaging identifies the fibrous cap in atherosclerotic abdominal aortic aneurysm. *Circulation* 109:1016–1021
- Kullo IJ, Edwards WD, Schwartz RS (1998) Vulnerable plaque: pathobiology and clinical implications. *Ann Intern Med* 129:1050–1060
- Lawrence JA, Kim D, Kent KC, Stehling MK, Rosen MP, Raptopoulos V (1995) Lower extremity spiral CT angiography versus catheter angiography. *Radiology* 194:903–908
- Le Gal G, Righini M, Roy PM, Sanchez O, Aujesky D, Bounameaux H, Perrier A (2006) Prediction of pulmonary embolism in the emergency department: the revised Geneva score. *Ann Intern Med* 144(3): 165–171
- Lederle FA, Johnson GR, Wilson SE et al (2002) Rupture rate of large abdominal aortic aneurysms in patients refusing or unfit for elective repair. *JAMA* 287:2968–2972
- Lenhart M, Framme N, Völk M, Strotzer M, Manke C, Nitz WR, Finkenzeller T, Feuerbach S, Link J (2002) Time-resolved contrast enhanced magnetic resonance angiography of the carotid arteries: diagnostic accuracy and inter-observer variability compared with selective catheter angiography. *Invest Radiol* 37(10):535–541
- Libby P (1998) The interface of atherosclerosis and thrombosis: basic mechanisms. *Vasc Med* 3:225–229
- Lovett JK, Gallagher PJ, Hands LJ, Walton J, Rothwell PM (2004a) Histological correlates of carotid plaque surface morphology on lumen contrast imaging. *Circulation* 110:2190–2197
- Lovett JK, Gallagher PJ, Rothwell PM (2004b) Reproducibility of histological assessment of carotid plaque: implications for studies of carotid imaging. *Cerebrovasc Dis* 18:117–123
- Mayo JR, Remy-Jardin M, Müller NL, Remy J, Worsley DF, Hossein-Foucher C, Kwong JS, Brown MJ (1997) Pulmonary embolism: prospective comparison of spiral CT with ventilation-perfusion scintigraphy. *Radiology* 205(2):447–452
- Mewhort HE, Appoo JJ, Sumner GL, Hergert E, Wong J (2011) Alternative surgical approach to repair of the ascending aorta. *Ann Thorac Surg* 92(3):1108–1110
- Minaker KL (2007) Common clinical sequelae of aging, Chap. 23. In: Goldman L, Ausiello D (eds) *Cecil medicine*, 23rd edn. Saunders/Elsevier, Philadelphia

- Mitsumori LM, Hatsukami TS, Ferguson MS, Kerwin WS, Cai J, Yuan C (2003) In vivo accuracy of multi-sequence MR imaging for identifying unstable fibrous caps in advanced human carotid plaques. *J Magn Reson Imaging* 17:410–420
- Moody AR, Murphy RE, Morgan PS (2003) Characterization of complicated carotid plaque with magnetic resonance direct thrombus imaging in patients with cerebral ischemia. *Circulation* 107:3047–3052
- Naghavi M, Libby P, Falk E et al (2003) From vulnerable plaque to vulnerable patient: a call for new definitions and risk assessment strategies. Part I. *Circulation* 108:1664–1672
- Naghavi M, Falk E, Hecht HS, Shah PK (2006) The first SHAPE (Screening for Heart Attack Prevention and Education) guideline. *Crit Pathw Cardiol* 5(4):187–190
- Nakazawa T, Watanabe Y, Hori Y, Kiso K, Higashi M, Itoh T, Naito H (2011) Lung perfused blood volume images with dual-energy computed tomography for chronic thromboembolic pulmonary hypertension: correlation to scintigraphy with single-photon emission computed tomography. *J Comput Assist Tomogr* 35(5):590–595
- Nandalur KR, Baskurt E, Hagspiel KD, Phillips CD, Kramer CM (2005) Calcified carotid atherosclerotic plaque is associated less with ischemic symptoms than is noncalcified plaque on MDCT. *AJR Am J Roentgenol* 184:295–298
- Nandalur KR, Hardie AD, Raghavan P, Schipper MJ, Baskurt E, Kramer CM (2007) Composition of the stable carotid plaque. Insights from a multidetector computed tomography study of plaque volume. *Stroke* 38:935–940
- Nederkoorn PJ, van der Graaf Y, Hunink MG (2003) Duplex ultrasound and magnetic resonance angiography compared with digital subtraction angiography in carotid artery stenosis: a systematic review. *Stroke* 34(5):1324–1332
- Nevitt MP, Ballard DJ, Hallett JW Jr (1989) Prognosis of abdominal aortic aneurysms. A population-based study. *N Engl J Med* 321:1009–1014
- Nienaber CA, Fattori R, Mehta RH, Richartz BM, Evangelista A, Petzsch M, Cooper JV, Januzzi JL, Ince H, Sechtem U, Bossone E, Fang J, Smith DE, Isselbacher EM, Pape LA, Eagle KA (2004) Gender-related differences in acute aortic dissection. *Circulation* 109(24):3014–3021
- Norman PE, Jamrozik K, Lawrence-Brown MM et al (2004) Population based randomised controlled trial on impact of screening on mortality from abdominal aortic aneurysm. *BMJ* 329:1259
- North American Symptomatic Carotid Endarterectomy Trial Collaborators (1991) Beneficial effect of carotid endarterectomy in symptomatic patients high with grade stenosis. *N Engl J Med* 325:445–453
- O'Rourke MF, Avolio AP, Lauren PD, Yong J (1987) Age-related changes of elastic lamellae in the human thoracic aorta. *J Am Coll Cardiol* 29:A53
- Ozkan U, Oğuzkurt L, Tercan F, Pourbagher A (2008) MRI and DSA findings in popliteal artery entrapment syndrome. *Diagn Interv Radiol* 14(2):106–110
- Parker DL, Yuan C, Blatter DD (1991) MR angiography by multiple thin slab 3D acquisition. *Magn Reson Med* 17:434–451
- Paterson JC (1938) Capillary rupture with intimal hemorrhage as a causative factor in coronary thrombosis. *Arch Pathol* 25:474–487
- Pieroni S, Foster BR, Anderson SW, Kertesz JL, Rhea JT, Soto JA (2009) Use of 64-row multidetector CT angiography in blunt and penetrating trauma of the upper and lower extremities. *Radiographics* 29(3):|863–876
- Polak JF, Kalina P, Donaldson MC (1993) Carotid endarterectomy: preoperative evaluation of candidates with combined Doppler sonography and MR angiography: work in progress. *Radiology* 186:333–338
- Prokop M (2003) General principles of MDCT. *Eur J Radiol* 45:S4–S10
- Prokop M, Shin HO, Schanz A, Schaefer-Prokop C (1997) Use of maximum intensity projections in CT angiography: a basic review. *Radiographics* 17:433–451
- Randoux B, Marro B, Koskas F (2001) Carotid artery stenosis: prospective comparison of CT, three-dimensional gadolinium-enhanced MR, and conventional angiography. *Radiology* 220:179–185
- Rankin SC (1998) Spiral CT: vascular applications. *Eur J Radiol* 28:18–29
- Razek AA, Saad E, Soliman N, Elatta HA (2010) Assessment of vascular disorders of the upper extremity with contrast-enhanced magnetic resonance angiography: pictorial review. *Jpn J Radiol* 28(2):87–94
- Reed WW, Hallett JW Jr, Damiano MA, Ballard DJ (1997) Learning from the last ultrasound: a population-based study of patients with abdominal aortic aneurysm. *Arch Intern Med* 157:2064–2068
- Reinartz P, Wildberger JE, Schaefer W, Nowak B, Mahnken AH, Buell U (2004) Tomographic imaging in the diagnosis of pulmonary embolism: a comparison between V/Q lung scintigraphy in SPECT technique and multislice spiral CT. *J Nucl Med* 45(9):1501–1508
- Remy-Jardin M, Remy J (2008) Vascular disease in chronic obstructive pulmonary disease. *Proc Am Thorac Soc* 5(9):891–899
- Remy-Jardin M, Remy J, Watinne L, Giraud F (1992) Central pulmonary thromboembolism: diagnosis with spiral volumetric CT with the single-breath-hold technique – comparison with pulmonary angiography. *Radiology* 185(2):381–387
- Remy-Jardin M, Remy J, Deschildre F, Artaud D, Beregi JP, Hossein-Foucher C, Marchandise X, Duhamel A (1996) Diagnosis of pulmonary embolism with spiral CT: comparison with pulmonary angiography and scintigraphy. *Radiology* 200(3):699–706
- Remy-Jardin M, Remy J, Mayo JR, Müller NL (2001) Pulmonary hypertension. In: *CT angiography of the chest*. Lippincott Williams & Wilkins, Philadelphia, pp 67–81

- Richardson M, Hatton MWC, Moore S (1988) Proteoglycan distribution in the intima and media of the aortas of young and aging rabbits: an ultrastructural study. *Atherosclerosis* 71:243–256
- Righini M, Le Gal G, Aujesky D, Roy PM, Sanchez O, Verschuren F, Rutschmann O, Nonent M, Cornuz J, Thys F, Le Manach CP, Revel MP, Poletti PA, Meyer G, Mottier D, Perneger T, Bounameaux H, Perrier A (2008) Diagnosis of pulmonary embolism by multidetector CT alone or combined with venous ultrasonography of the leg: a randomised non-inferiority trial. *Lancet* 371(9621):1343–1352
- Ritchie G, McGurk S, McCreath C, Graham C, Murchison JT (2007) Prospective evaluation of unsuspected pulmonary embolism on contrast enhanced multidetector CT (MDCT) scanning. *Thorax* 62:536–540
- Robert L, Jacob MP, Frances C, Godeau G, Hornebeck W (1984) Interaction between elastin and elastases and its role in aging of arterial wall, skin, and other connective tissues. A review. *Mech Ageing Dev* 28:155–166
- Rothwell PM, Gibson R, Warlow CP (2000) Interrelation between plaque surface morphology and degree of stenosis on carotid angiograms and the risk of ischemic stroke in patients with symptomatic carotid stenosis. *Stroke* 31:615–621
- Rubin GD, Dake MD, Semba CP (1995) Current status of three-dimensional spiral CT scanning for imaging the vasculature. *Radiol Clin North Am* 33:51–70
- Rubin GD, Shiau MC, Schmidt AJL et al (1999) Computed tomographic angiography: historical perspective and new state-of-the-art using multidetector helical computed tomography. *J Comput Assist Tomogr* 23(Suppl 1):S83–S90
- Saam T, Cai J, Ma L, Cai YQ, Ferguson MS, Polisser NL, Hatsukami TS, Yuan C (2006) Comparison of symptomatic and asymptomatic atherosclerotic carotid plaque features with in vivo MR imaging. *Radiology* 240:464–472
- Saam T, Hatsukami TS, Takaya N (2007) The vulnerable, or high risk atherosclerotic plaque: noninvasive MR imaging for characterization and assessment. *Radiology* 244:64–77
- Saba L, Mallarini G (2009a) Update on Carotid Artery. *Imaging Ital J Vasc Endovasc Surg* 16:203–221
- Saba L, Mallarini G (2009b) Fissured fibrous cap of vulnerable carotid plaques and symptomaticity: are they correlated? Preliminary results by using MDCTA. *Cerebrovasc Dis* 27:322–327
- Saba L, Mallarini G (2010a) A comparison between NASCET and ECST methods in the study of carotids: evaluation using Multi-Detector-Row CT angiography. *Eur J Radiol* 76(1):42–47
- Saba L, Mallarini G (2010b) Comparison between quantification methods of carotid artery stenosis and computed tomographic angiography. *J Comput Assist Tomogr* 34(3):421–430
- Saba L, Caddeo G, Sanfilippo R, Montisci R, Mallarini G (2007a) CT and US in the study of ulcerated carotid plaque compared with surgical results. Advantages of multi-detector-row CT angiography. *AJNR Am J Neuroradiol* 28:1061–1066
- Saba L, Caddeo G, Sanfilippo R, Montisci R, Mallarini G (2007b) CT and ultrasound in the study of ulcerated carotid plaque compared with surgical results: potentialities and advantages of multidetector row CT angiography. *AJNR Am J Neuroradiol* 28(6):1061–1066
- Saba L, Caddeo G, Sanfilippo R, Montisci R, Mallarini G (2007c) Efficacy and sensitivity of axial scans and different reconstruction methods in the study of the ulcerated carotid plaque using multidetector-row CT angiography: comparison with surgical results. *AJNR Am J Neuroradiol* 28(4):716–723
- Saba L, Montisci R, Sanfilippo R, Mallarini G (2009) Multidetector Row CT of the brain and carotid artery: a correlative analysis. *Clin Radiol* 64:767–778
- Sacco RL, Adams R, Albers G (2006) Guidelines for prevention of stroke in patients with ischemic stroke or transient ischemic attack. *Stroke* 37:577–617
- Sadowski EA, Bennett LK, Chan MR et al (2007) Nephrogenic systemic fibrosis: risk factors and incidence estimation. *Radiology* 243(1):148–157, Epub 2007 Jan 31
- Sameshima T, Futami S, Morita Y, Yokogami K, Miyahara S, Sameshima Y et al (1999) Clinical usefulness and problems with three-dimensional CT angiography for the evaluation of atherosclerotic stenosis of the carotid artery: comparison with conventional angiography, MRA and ultrasound sonography. *Surg Neurol* 51:300–309
- Schwartz JB, Zipes DP (2007) Cardiovascular disease in the elderly: Chap. 75. In: Libby P, Bonow RO, Mann DL, Zipes DP (eds) *Braunwald's heart disease: a textbook of cardiovascular medicine*, 8th edn. Saunders/Elsevier, Philadelphia
- Schwartz RB, Jones KM, Chernoff DM et al (1992) Common carotid artery bifurcation: evaluation with spiral CT. *Radiology* 185:513–519
- Schwicker HC, Schweden F, Schild HH et al (1994) Pulmonary arteries and lung parenchyma in chronic pulmonary embolism: preoperative and postoperative CT findings. *Radiology* 191(2):351–357
- Schwoppe RB, Alper HJ, Talenfeld AD, Cohen EI, Lookstein RA (2007) MR angiography for patient surveillance after endovascular repair of abdominal aortic aneurysms. *AJR Am J Roentgenol* 188(4):W334–W340
- Seeger MD, Barratt BS, Lawson GA, Klingman N (1995) The relationship between carotid plaque composition, morphology, and neurological symptoms. *J Surg Res* 58:330–336
- Selvin E, Erlinger TP (2004) Prevalence of and risk factors for peripheral arterial disease in the United States: results from the National Health and Nutrition Examination Survey, 1999–2000. *Circulation* 110(6):738–743, Epub 2004 Jul 19
- Simonneau G, Galè N, Rubin LJ, Langleben D, Seeger W, Domenighetti G, Gibbs S, Lebrec D, Speich R, Beghetti M, Rich S, Fishman A (2004) Clinical classification of pulmonary hypertension. *J Am Coll Cardiol* 43(12 Suppl S):5S–12S

- Stein PD, Henry JW, Relyea B (1995) Untreated patients with pulmonary embolism. Outcome, clinical, and laboratory assessment. *Chest* 107(4):931–935
- Sztajzel R, Momjian S, Momjian-Mayor I, Murih N, Djebaili K, Boissard M et al (2005) Stratified gray scale median analysis and color mapping of the carotid plaque: correlation with endarterectomy specimen histology of 28 patients. *Stroke* 36:741–745
- Tahara S, Bezerra HG, Sirbu V, Kyono H, Musumeci G, Rosenthal N, Guagliumi G, Costa MA (2010) Angiographic, IVUS and OCT evaluation of the long-term impact of coronary disease severity at the site of overlapping drug-eluting and bare metal stents: a sub-study of the ODESSA trial. *Heart* 96(19):1574–1578
- Tahmasebpour HR, Buckley AR, Cooperberg PL, Fix CH (2005) Sonographic examination of the carotid arteries. *Radiographics* 25(6):1561–1575
- Tapson VF (2008) Acute pulmonary embolism. *N Engl J Med* 358:1037–1052
- Tawakol A, Migrino RQ, Bashian GG, Bedri S, Vermylen D, Cury RC, Yates D, LaMuraglia GM, Furie K, Houser S, Gewirtz H, Muller JE, Brady TJ, Fischman AJ (2006) In vivo 18F-fluorodeoxyglucose positron emission tomography imaging provides a noninvasive measure of carotid plaque inflammation in patients. *J Am Coll Cardiol* 48(9):1818–1824
- Toussaint JF, LaMuraglia GM, Southern JF, Fuster V, Kantor HL (1996) Magnetic resonance images lipid, fibrous, calcified, hemorrhagic, and thrombotic components of human atherosclerosis in vivo. *Circulation* 94(5):932–938
- Towfighi A, Saver JL (2011) Stroke declines from third to fourth leading cause of death in the United States: historical perspective and challenges ahead. *Stroke* 42(8):2351–2355
- Truijers M, Fütterer JJ, Takahashi S, Heesakkers RA, Blankensteijn JD, Barentsz JO (2009) In vivo imaging of the aneurysm wall with MRI and a macrophage-specific contrast agent. *AJR Am J Roentgenol* 193(5):W437–W441
- U-King-Im JM, Fox AJ, Aviv RI, Howard P, Yeung R, Moody AR, Symons SP (2010) Characterization of carotid plaque hemorrhage: a CT angiography and MR intraplaque hemorrhage study. *Stroke* 41(8):1623–1629
- Verhoek G, Costello P, Khoo EW, Wu R, Kat E, Fitridge RA (1999) Carotid bifurcation CT angiography: assessment of interactive volume rendering. *J Comput Assist Tomogr* 23:590–596
- Virmani R, Avolio AP, Mergner WJ et al (1991) Effect of aging on aortic morphology in populations with high and low prevalence of hypertension and atherosclerosis. Comparison between occidental and Chinese communities. *Am J Pathol* 139:1119–1129
- Waki H, Masuyama T, Mori H, Maesa T, Kitade K, Moriyasu K, Tsujimoto M, Fujimoto K, Koshimae N, Masuura N (2003) Ultrasonic tissue characterization of the atherosclerotic carotid artery. *Circulation* 67:1013–1016
- Walker LJ, Ismail A, McMeekin W, Lambert D, Mendelow AD, Birchall D (2002) Computed tomography angiography for the evaluation of carotid atherosclerotic plaque: correlation with histopathology of endarterectomy specimens. *Stroke* 33:977–981
- Walter D, De Man B, Iatrou M, Edic PM (2004) Future generation CT imaging. *Thorac Surg Clin* 14:135–149
- Wasserman BA, Smith WI, Trout HH III, Cannon RO 3rd, Balaban RS, Arai AE (2002) Carotid artery atherosclerosis: in vivo morphologic characterization with gadolinium enhanced double-oblique MR imaging-initial results. *Radiology* 223:566–573
- Wehrli FW, Shimakawa A, Gullberg GT, MacFall JR (1986) Time-of-flight MR flow imaging: selective saturation recovery with gradient refocusing. *Radiology* 160:781–785
- Weinberger J (2002) Prevention of ischemic stroke. *Curr Treat Options Cardiovasc Med* 4(5):393–403
- Weishaupt D, Rühm SG, Binkert CA, Schmidt M, Patak MA, Steybe F, McGill S, Debatin JF (2000) Equilibrium-phase MR angiography of the aortoiliac and renal arteries using a blood pool contrast agent. *AJR Am J Roentgenol* 175(1):189–195
- Wells PS, Ginsberg JS, Anderson DR, Kearon C, Gent M, Turpie AG, Bormanis J, Weitz J, Chamberlain M, Bowie D, Barnes D, Hirsh J (1998) Use of a clinical model for safe management of patients with suspected pulmonary embolism. *Ann Intern Med* 129(12):997–1005
- Willmann JK, Wildermuth S, Pfammatter T, Roos JE, Seifert B, Hilfiker PR, Marincek B, Weishaupt D (2003) Aortoiliac and renal arteries: prospective intraindividual comparison of contrast-enhanced three-dimensional MR angiography and multi-detector row CT angiography. *Radiology* 226(3):798–811
- Wintermark M, Jawadi SS, Rapp JH, Tihan T, Thong E, Glidden DV (2008a) High resolution CT imaging of carotid artery atherosclerotic plaques. *AJNR Am J Neuroradiol* 29:875–882
- Wintermark M, Jawadif SS, Rappe JH, Tihan T, Tonga E, Glidden DV et al (2008b) High-resolution CT images of carotid artery atherosclerotic plaque. *AJNR Am J Neuroradiol* 29:875–882
- Wintermark M, Arora S, Tong E, Vittinghoff E, Lau BC, Chien JD, Dillon WP, Saloner D (2008c) Carotid plaque computed tomography imaging in stroke and non-stroke patients. *Ann Neurol* 64:149–157
- Wintermark M, Jawadi SS, Rapp JH, Tihan T, Tong E, Glidden DV et al (2008d) High resolution CT imaging of carotid artery atherosclerotic plaques. *AJNR Am J Neuroradiol* 29:875–882
- Wong DD, Ramaseshan G, Mendelson RM (2011) Comparison of the Wells and Revised Geneva Scores for the diagnosis of pulmonary embolism: an Australian experience. *Intern Med J* 41(3):258–263
- Yuan C, Mitsumori LM, Beach KW, Maravilla KR (2001) Carotid atherosclerotic plaque: non invasive MR characterization and identification of vulnerable lesions. *Radiology* 221:285–299
- Yucel EK, Anderson CM, Edelman RR et al (1999) Magnetic resonance angiography. Update on applications for extracranial arteries. *Circulation* 100:2284–2301